EUR 3920 e

EUROPEAN ATOMIC ENERGY COMMUNITY - EURATOM

HEAT TRANSFER CRISIS WITH STEAM-WATER MIXTURES IN ROUND CONDUITS: REPRODUCIBILITY TESTS WITH DIFFERENT EXPERIMENTAL FACILITIES

by

A. HASSID, A. MILANI, R. RAVETTA and L. RUBIERA
(CISE)

1968

CIRENE Program

Report prepared by CISE
Centro Informazioni Studi Esperienze, Segrate (Milan) - Italy

Euratom/CNEN/CISE Contract No. 008-65-1 NTRI

LEGAL NOTICE

This report is on sale at the addresses listed on cover page 4

at the price of FF 10.–	FB 100.–	DM 8.–	Lit. 1.250	Fl. 7.25

When ordering, please quote the EUR number and the title, which are indicated on the cover of each report.

Printed by SMEETS
Brussels, May 1968

EUR 3920 e

HEAT TRANSFER CRISIS WITH STEAM-WATER MIXTURES IN ROUND CONDUITS : REPRODUCIBILITY TESTS WITH DIFFERENT EXPERIMENTAL FACILITIES
by A. HASSID, A. MILANI, R. RAVETTA and L. RUBIERA (CISE)

European Atomic Energy Community - EURATOM
CIRENE Program
Report prepared by CISE - Centro Informazioni Studi Esperienze, Segrate (Milan) - Italy
Euratom/CNEN/CISE Contract No. 008-65-1 NTRI
Brussels, May 1968 - 76 Pages - 29 Figures - FB 100

This report presents a comparison between heat transfer crisis data with vertical upward flow of steam-water mixtures in round tubes, obtained with different experimental plants.

EUR 3920 e

HEAT TRANSFER CRISIS WITH STEAM-WATER MIXTURES IN ROUND CONDUITS : REPRODUCIBILITY TESTS WITH DIFFERENT EXPERIMENTAL FACILITIES
by A. HASSID, A. MILANI, R. RAVETTA and L. RUBIERA (CISE)

European Atomic Energy Community - EURATOM
CIRENE Program
Report prepared by CISE - Centro Informazioni Studi Esperienze, Segrate (Milan) - Italy
Euratom/CNEN/CISE Contract No. 008-65-1 NTRI
Brussels, May 1968 - 76 Pages - 29 Figures - FB 100

This report presents a comparison between heat transfer crisis data with vertical upward flow of steam-water mixtures in round tubes, obtained with different experimental plants.

The experiments were carried out under the following conditions :

- geometry : round tube I.D. = 2.5 cm; L = 240 cm and 160 cm
- specific mass flowrate : $G = 40 \div 380$ g/cm²s
- pressure : $P = 30; 50; 60$ kg/cm²
- inlet quality : $-0.30 \leqslant X_{in} \leq 0.$

The experimental plants CISE IETI-2 and IETI-3 and SORIN high pressure facility are briefly described.

The results, obtained with the same test element, are generally in good agreement, but under some conditions, still unexplained discrepancies are evident. This is in agreement with the observations made by other researchers, with both round ducts and rod bundles.

The discrepancies are analyzed and a margin of uncertainty is derived for the critical power values.

The experiments were carried out under the following conditions :

- geometry : round tube I.D. = 2.5 cm; L = 240 cm and 160 cm
- specific mass flowrate : $G = 40 \div 380$ g/cm²s
- pressure : $P = 30; 50; 60$ kg/cm²
- inlet quality : $-0.30 \leqslant X_{in} \leq 0.$

The experimental plants CISE IETI-2 and IETI-3 and SORIN high pressure facility are briefly described.

The results, obtained with the same test element, are generally in good agreement, but under some conditions, still unexplained discrepancies are evident. This is in agreement with the observations made by other researchers, with both round ducts and rod bundles.

The discrepancies are analyzed and a margin of uncertainty is derived for the critical power values.

EUR 3920 e

EUROPEAN ATOMIC ENERGY COMMUNITY - EURATOM

HEAT TRANSFER CRISIS WITH STEAM-WATER MIXTURES IN ROUND CONDUITS:
REPRODUCIBILITY TESTS WITH DIFFERENT EXPERIMENTAL FACILITIES

by

A. HASSID, A. MILANI, R. RAVETTA and L. RUBIERA
(CISE)

1968

CIRENE Program

Report prepared by CISE
Centro Informazioni Studi Esperienze, Segrate (Milan) - Italy

Euratom/CNEN/CISE Contract No. 008-65-1 NTRI

SUMMARY

This report presents a comparison between heat transfer crisis data with vertical upward flow of steam-water mixtures in round tubes, obtained with different experimental plants.

The experiments were carried out under the following conditions :

- geometry : round tube I.D. = 2.5 cm; L = 240 cm and 160 cm
- specific mass flowrate : $G = 40 \div 380$ g/cm^{2}s
- pressure : $P = 30; 50; 60$ kg/cm^2
- inlet quality : $-0.30 \leqslant X_{in} \leq 0.$

The experimental plants CISE IETI-2 and IETI-3 and SORIN high pressure facility are briefly described.

The results, obtained with the same test element, are generally in good agreement, but under some conditions, still unexplained discrepancies are evident. This is in agreement with the observations made by other researchers, with both round ducts and rod bundles.

The discrepancies are analyzed and a margin of uncertainty is derived for the critical power values.

KEYWORDS

HEAT TRANSFER	TUBES
FLUID FLOW	TWO-PHASE FLOW
STEAM	BURNOUT
WATER COOLANT	DEPARTURE NUCLEATE BOILING

TABLE OF CONTENTS

HEAT TRANSFER CRISIS WITH STEAM-WATER MIXTURES IN ROUND CONDUITS: REPRODUCIBILITY TESTS WITH DIFFERENT EXPERIMENTAL FACILITIES (+)

1. INTRODUCTION

1.1. In the design of water cooled reactors (BWR, SGHWR, CIRENE, etc.) a most important parameter which conditions their performance limits and therefore their economics is heat transfer crisis (often called "burn-out" or "dry-out" or "departure from nucleate boiling" (DNB)).

With this purpose, designers generally make use of empirical or semi empirical correlations for predicting critical power under design conditions. In order to establish the safety margin with respect to the crisis, they evidently need to know the reliability degree of these correlations, a parameter which, in certain cases, may have a great economic impact on a reactor system. The question has been treated during the latest European Two-Phase Heat Transfer Meeting at Bournemouth (U.K.)[15] and the statement has been generally accepted that reactor designers "expect that the correlations will be presented accompanied by recommendations and precise comments, indicating the anticipated scatter according to the various ranges of working conditions".

1.2. In the critical power correlation inaccuracy, the following factors are present:

i) the experimental points from which the correlations are derived are affected by accidental errors due to the inaccuracy of the measurement apparatus;

ii) the experimental points are scattered for unknown reasons (due, for example, to an "experimental plant effect" or to a "test element building effect");

iii) the correlation does not give an exact description of the phenomenology and, under certain conditions it does not give the exact dependence of the governing parameters.

The most recent correlations, which are now being widely used, take into account all these factors by giving a certain statistics of the errors. For example:

(+) Manuscript received on March 1, 1968.

- CISE correlation for round tubes[7]: 84% of the data are predicted within ± 15% in the range of validity;
- CISE correlation for rod bundles and annuli[7]: 67%, 81% and 90% of the data are predicted within ± 15%, ± 20%, ± 25% respectively;
- Macbeth correlation for rod bundles[14]: 6.1% RMS error and 97% of the experimental results are predicted within ± 12%;
- Barnett correlation for rod bundles and annuli[17]: 6.7% RMS error;
- Becker correlation[18]: ± 3.8% RMS error for the Swedish data scatter for data of various origins ranges from - 10% to + 23% (for rod bundles).

Usually in the most recent systematic data published in the literature, the factor inherent to point i) is much smaller than the overall inaccuracy stated for the correlations. Improvements in the correlations could be obtained by reducing the inaccuracy up to the one due to factor ii). An accurate determination of factor ii) seems to be therefore quite important.

1.3. This problem has been tackled at the Winfrith laboratories by Lee[11] and by Stevens and Wood[19].

Lee measured critical power in the same test element with different plants and discrepancies were found up to 10% (± 5% around a mean value). No satisfactory explanation could be offered at that time for these discrepancies.

Stevens and Wood[19], in carrying out experiments with the same rod bundle but with successive rebuilding in a freon experimental plant, found a repeatibility not better than ± 6% around a mean value. Again no satisfactory explanation was found.

1.4. In the occasion of the commissioning and first heat transfer tests with the CISE IETI-3 experimental plant in Piacenza[4], a set of repeatibility runs was carried out with the same test element and under the same experimental conditions as those investigated with the CISE IETI-2 plant, formerly located at the Stabilimento Meccanico Ansaldo in Genoa[2].

The test element was a 2.5 cm I.D. tube and the new results showed a significant discrepancy (critical power values were larger) with respect to the previous ones.

It seemed therefore necessary to carry out a systematic investigation for determining, at least for a circular tube, the critical power repeatibility. The investigation should have involved the largest number of experimental plants: also the SORIN facility, which has the advantage of being quite different from the CISE plants, was thus used.

From all the accumulated results a figure has been derived for the uncertainty of the data which can be reasonably considered as the minimum error band for critical power correlations.

2. EXPERIMENTAL PLANTS AND INSTRUMENTATION

The data relevant to three different experimental facilities are described and analyzed: a description of the three plants (CISE IETI-2 (Genoa), CISE IETI-3 (Piacenza), SORIN (Saluggia)) is given here below.

2.1. CISE IETI-2 Plant (Genoa)

2.1.1. An exhaustive description of this plant - which was dismantled in September 1965 - can be found in ref. 2. A schematic diagram of the facility and of the hydraulic section with the related instrumentation is given in figs. 1 and 2.

Superheated steam (up to 350 °C and 62 kg/cm^2) was supplied by an oil fired boiler; degassified and demineralized water[(+)] at high pressure (up to 71 kg/cm^2 abs) was supplied by feed pumps located upstream of the boiler. Two different lines brought steam and subcooled water to the test assembly: a desuperheater and a series of orifices for flowrate measurements were inserted in the steam line; a water preheater and a similar flowrate measurement system were inserted in the water line. Pneumatic valves operated on the inlet water line and on the steam side of the water preheaters.

The test assembly consisted of an interchangeable mixer[(3)], the vertical test section and a separator. In the case of subcooled water at the inlet, the mixer could be substituted with a throttling valve.

A pressure control valve was located downstream of the separator on the steam line, leading to a cooled sea-water condenser. From the separator the water line led to a tank, where the water level was automatically controlled by a depressurizing valve, then to a second separator and finally to a condenser-cooler similar to that on the steam line.

(+) Checks of the water analysis made from time to time showed that water purity was poor (~ 360 μs/cm conductivity) though it matched the requirements of the boiler and the plant components.

Water from the two condenser-coolers was eventually discharged into a reservoir and sent to the waste.

The piping and plant components were made of carbon steel, with the exception of the test assembly (stainless steel).

Test elements were heated by Joule effect by means of a d.c. generators set. Power was supplied directly from the 12 kV medium voltage network of the factory; two transformers lowered the voltage to 220 V to feed the motors of 28 d.c. conventional welding machines, divided into seven groups of 4 generators, working in parallel or in series two by two.

The excitation current of the seven groups of rotating d.c. generators was regulated by means of rheostats in series with each excitation circuit for a fine control of the test element power. Power to the test section could be shorted if necessary by short circuit switches.

The rating of the experimental plant was:

- steam line: normal operating pressure 51 kg/cm^2 abs, maximum flowrate 8 t/h at a maximum temperature of 360 °C;
  Rating pressure of the boiler (nominal thermal power 9 MW): 61 kg/cm^2 abs.
- Water-line: maximum flowrate 10 t/h at a temperature varying from 120 °C to slightly subcooling for a maximum operating pressure of 71 kg/cm^2 abs (in subcooled test section inlet conditions).
- Maximum d.c. power to the test element: continuous service 0.5 MW, peak service 1 MW.

2.1.2. The measured quantities for each heat transfer crisis experiment were: inlet flowrates and enthalpies of both phases, power to the test section, pressures and possibly the pressure drop across the test element.

The flowrates of (slightly superheated) steam and subcooled water were measured just upstream of the mixer by means of orifice flowmeters, calibrated from time to time to give a minimum accuracy of $\pm$ 3.5% for steam and $\pm$ 1 ÷ 2% for water flowrates.

The d.c. power supplied to the test section was measured by means of a 0.5 class millivoltmeter (current measurement) and a 0.5 class voltmeter (voltage measurement): the total power measurement accuracy was within ± 2 ÷ 3%.

Pressures were measured at different points by means of steel blade manometers of the Blondelle type, (0 ÷ 100 kg/cm^2 f.s.) calibrated from time to time; the accuracy was ± 2% full scale.

A high pressure differential manometer (mercury filled U tube, 2000 mm Hg. f.s.) measured the pressure drop across the test section with a ± 2% accuracy.

The inlet enthalpy was obtained from the water or steam temperature measured by Ni-NiCr thermocouples, whose hot junctions were located in stainless steel jackets, plunged into the water and steam lines. The total error of the temperature measurement was estimated to be about ± 3°C; in the case of inlet subcooled conditions, this means an enthalpy measurement accuracy within ± 3 ÷ 5 kcal/kg, while for two-phase inlet conditions the inlet enthalpy error could amount to 7 ÷ 14 kcal/kg.

For a detailed analysis of the error evaluation see(2).

2.1.3. The heat transfer crisis was detected by a differential thermocouple located upstream of the power lug of EL G1(3).

Burn out detectors were also employed as safety devices(3) (zinc strip or bridge electrical detector, operating the short circuit switch).

2.2. CISE IETI-3 Plant (Piacenza)

2.2.1. A provisional description of this new facility which substitutes the IETI-2 plant and is installed at the ENEL "Emilia" power station in Piacenza, can be found in(4). A diagram of the hydraulic circuit and the test section power supply system is given in Figs. 3 and 4.

The rating of the plant is:

water flowrate	40 m^3/h
steam flowrate	10 t/h
pressure at the test assembly	60 kg/cm^2
d.c. power	7 MW full service.

In order to obtain the required inlet enthalpy of the mixture at high mass flowrate, the flow sheet of the IETI-2 plant had to be changed and water recirculation adopted for a partial heat recovery.

Therefore, according to the required flowrate, the plant is operated either as an open circuit (see Fig. 5-a, up to 20 t/h) or as a "semiopen" circuit (see Fig. 5-b), for which water is recirculated for a partial heat and flowrate recovery ($\Gamma \gtrsim 20$ t/h)(+).

Superheated steam is drawn from the intermediate superheaters of the two station boilers at 105 kg/cm^2 and 430 °C: steam is used for the following three purposes:

- degassifying the feeding water;
- preheating the circulating water;
- feeding the test section in the case of two-phase inlet conditions.

As shown in Figs. 3 or 5, demineralized water, taken from a reservoir (~ 80 m^3) is sent into a degassifier (temperature: 105 °C, pressure: 1.2 kg/cm^2 abs.) and then brought to high pressure by two reciprocating pumps in parallel (head: 120 kg/cm^2, flowrate 20 m^3/h each(°)). Water is then sent through three heat exchangers. In the first heat is supplied by the water leaving the separator downstream of the test section; in the second (recovered from the Genoa plant) and in the third, heat is transferred from superheated (in the latter exchanger) and condensing steam (in the former) coming from the boiler (when the plant is operated as an open circuit, the circulating water by-passes preheater N. 1, (Fig. 5a)). Water is finally sent to the flowmeter orifices and a mixer just upstream of the test section.

(+) All the experiments described in the present report were carried out without recirculation and for subcooled inlet conditions.

(°) The head of the pumps, with only slight modifications, can be increased up to even 400 kg/cm^2 (with a reduction in flowrate).

For water degassifying steam is depressurized through an automatic pneumatic valve controlled by the degassifier pressure.

For water preheating steam is throttled through a pneumatic valve, handly controlled and the condensate is discharged into the low pressure separator and then into the condenser.

For test section feeding steam goes through a desuperheater (recovered from the Genoa plant), where water coming from the pumps is injected and is eventually sent to the test section through the flowmeter orifices.

Experiments with two or single phase flow at the test element entrance are therefore possible.

The steam-water mixture leaving the test section enters a separator where the two phases are sent to their own lines. Steam is depressurized through a throttling valve, automatically or manually operated to keep the pressure at the test element outlet constant(+) and then sent to the condenser (recovered from the Genoa plant). Water is discharged into a "level thank", it goes through preheater N. 1 and then is depressurized through an automatic valve which keeps the level steady in the thank.

Downstream of the depressurizing valve, water can be discharged either into a low pressure separator and then into the condensers--coolers, river water cooled, if the plant is operated as an open circuit, or directly into the degassifier when the loop is partially closed (Fig. 5-b).

The change between the operating schemes a and b, (Fig. 5) is quite simply carried out by means of valves(°).

(+) When experiments at a mass flowrate much lower than the rated value and with subcooled water at the inlet are carried out, the pressure of the circuit is kept constant by operating manually a small valve on the water line downstream of the separator. This is the case of many experiments here presented.

(°) The loop operation, when the station boilers are shut down and no high pressure steam is available, is made possible with total heat recovery and water recirculation (thermally closed loop). An already existing Sulzer boiler (~ 2 MW), used by ENEL to start the station boilers, provides steam at 12 kg/cm^2 to feed the water degassifier. An additional electrical preheater has been necessively installed on the water line upstream of the test section for a fine regulation of the inlet temperature (subcooled inlet) and possibly to obtain two-phase inlet conditions.

The demineralized water provided by the station facilities is filtered in an ion axchanger resin bed downstream of the degassifier and its pH value is controlled with hydrazine injection. Net filters are fitted at various points of the loop to stop solid particles coming from carbon steel erosion.

After some time of operation without special control of water purity, remarkable deposit of iron oxide (red hematite) was found in all plant components (see 6.1.). Therefore accurate washing and pickling of the whole circuit was carried out with a warm acid solution (~ 80 °C, pH 3.6).

Alkaline passivation with warm solution (80 °C, pH 9.2) was then carried out to obtain a stable oxide layer (black magnetite) on the surfaces of the components and pipings of the plant.

When the loop is stopped after each daily operation, the plant is filled up with cold water in order to minimize contact with the atmosphere; on the average the chemical analysis of the circulating water is:

Electrical conductivity	7.5 μS/cm
pH (at room temperature)	9.2
Alkalinity	M = 3, P = 1 γ/liter
SiO_2	120 γ/liter
NH_3	220 "
N_2H_4	360 "
Fe	640 "
Cu	26 "
O_2	nil

The pH value (daily checked) is controlled with calibrated injection of hydrazine solution by means of a dosimetric pump upstream of the resin ion exchanger.

2.2.2. Electric power (Fig. 4) for the plant operation and element heating is supplied at 3,000 V by an already installed transformer (130,000/ /3000 V, 10,000 KVA, 50 Hz), normally utilized by ENEL for the station utilities. The secondary of the transformer feeds two different lines through two circuit breakers: the first (1,200 A) is installed on the line feeding a 6 MW d.c. static generator group for test element heating; the second is installed on a line (300 A) feeding two transformers. The first (3,000/380 V, Y/Y, 400 KVA, 50 Hz) supplies power for the plant utilities and the second (300/380 V, Y/Δ, 1,050 KVA, 50 Hz) supplies power to the d.c. rotating generators (recovered from the Genoa plant) for test element heating.

The d.c. generator group(+) consists of a variable ratio transformer (8,200 KVA nom; 3,000/0 ÷ 6,000 V in 60 steps) and of a double core transformer (6,000/100 V) fed from the secondary of the variable ratio transformer. The whole unit feeds two identical d.c. static generators (silicon diodes) which can be operated in parallel or in series (according to the electrical resistance of the test element) and have the following characteristics; voltage 100 V - current 25,000 A - power 2,5 MW.

The variable ratio transformer is however provided with additional taps in order to enlarge the transformation ratio to 3,000/0-7,200 V. In this case the two units have the following characteristics: 120 V - 25,000 A and the available d.c. power is increased to 6 MW (this operation can be tolerated for a 3 h duty). Control of the d.c. static generator power is achieved by means of the above mentioned variable ratio transformer (60 steps of 1.5 V) and of saturable reactors for fine control (over 5 steps of the transformer).

Summarizing, the available power for test element heating is:

	static generator	rotating generator	overall
full service	5 MW-2x (100 V-25,000 A)	0.45MW-24x(39 V-480 A)	5.45 MW
peak service (3 hours)	6 MW-2x (120 V-25,000 A)	" "	6.45 MW
peak service (few min.)	" "	0.95MW-24x(50 V-800 A)	6.95 MW

The power shut-off is carried out by means of a short-circuit switch for the rotating generators and of the high voltage circuit breaker

(+) The static generator has been available since March 1967; therefore only the rotating generators were used for the experiments carried out with EL G1 (Oct. 1966) and IT 18 (Jan.-Feb. 1967).

(primary of the 10 MVA transformer) for the static generator.

2.2.3. For the instrumentation accuracy reference is made to 2.1.2 because most of the measuring instruments of the IETI-3 plant have been recovered from the dismantled IETI-2. However improvements have been achieved in the thermocouple instrumentation and the total error of temperature measurements of water and steam upstream of the test section can now be estimated to be ± 1.5 °C; therefore the inlet enthalpy value is more reliable than stated in 2.1.2 (± 2 kcal/kg for subcooled inlet, ~ ± 5 kcal/kg for two-phase inlet)(+).

2.2.4. The test section instrumentation was:

a) for EL G1, tested in Oct. 1966, see 2.1.3.
b) EL IT18, tested in Jan.-Feb. 1967, and EL IT22 tested in May 1967, were equipped with a "thermocoax" thermocouple plunged into the inlet calming section to measure the water temperature, with two thermocouples at the outlet to detect the crisis, and with a resistance bridge type burnout detector. In this device (Fig. 6) the bridge unbalance signal, brought about by the onset of the crisis enters a balanced amplification stage. The output is sent to a relay operating a warning light(°) and to a further amplification stage eventually operating the trip of the test element power within a few ms.

2.3. SORIN High Pressure Facility (Saluggia)

2.3.1. A detailed description of the circuit is given in Ref. 8. Unlike the CISE plants, the hydraulic circuit (Fig. 7) is a closed loop of approximately 150 liters volume completely made of AISI 304 stainless steel. Water at high pressure and temperature is circulated by a zero leakage pump, (max. temperature 340 °C, max. pressure ~ 175 kg/cm^2, max.

(+) These figures concern the experiments carried out on EL IT18 and IT22 (Tables 3 to 6).

(°) To single out the rod on which the crisis sets in, when a single detector for each rod is used in rod bundles.

flowrate 36 m^3/h against 100 m head), and the heat transferred to the water in the loop is removed by a cooler system (~ 600 kW) located on the suction side of the pump. This provides a coarse control of the inlet subcooling, while a fine adjustement is achieved by means of an electric preheater upstream of the test section (40 kW). The test element is heated by Joule effect by means of direct current supplied from a d.c. rectifier unit capable of delivering 600 kW at 5,000 A (continuous operation) with 30% overload for short time operation (~ 15 min.).

The voltage control set, consisting of booster transformers fed by autotrasformers, allows a continuous regulation from 5 to 120 V. The circuit breaker (60 ms shut-off time) actuated by the burn-out detector is installed in the 6.000 V supply of the main transformer.

A pressurizer (100 liter volume) is connected with the loop at the test channel outlet to allow thermal expansion of the fluid and pressure stabilization. Degassfying of the coolant is obtained by recirculating water through an electrically heated degassifier, to achieve a maximum oxygen concentration of 0.14 ppm. Water make-up is provided by means of a mixed bed type deionizing unit to fulfill the requirement of 2 μs/cm(+) maximum conductivity. A 2" by-pass, in parallel to the vertical test section, provides a mixing of the steam-water mixture and of the by-pass water at the test section outlet(o).

2.3.2. The water flowrate into the test section is measured by an orifice plate, connected with a direct reading high pressure glass manometer, as well as by a Faure Hermann turbine type flowmeter, located at the entrance,

(+) Water chemical analysis :

Electrical conductivity	1,6 μs/cm
pH (at room temperature)	8.3
Alkalinity	3 γ/liter
SiO_2	45 "
NH_3	20 "

(o) On the CISE plants on the contrary, the test assembly outlet consisted of a piping (D = 2.5 cm, L ≈ 3 ÷ 4 m) connecting the test element flange with the separator.

whose signal is continuously recorded. The total error is ± 1.5%.

The electric power to the test section is measured by means of 0.5 class instruments; the total error ranges from ± 1.5% to ± 3%, going from higher to lower power values respectively.

Static pressure is measured with a Bourdon gage calibrated from time to time within a ± 0.5 kg/cm^2 accuracy. Pressure drops are measured by means of differential transducers of S.E.L. reluctance type, whose signal is detected by a potentiometer recorder. The overall estimated error is ± 3%.

Temperatures at the heated channel inlet and exit are measured by means of stainless steel jacketed calibrated thermocouples (Chromel--Alumel "thermocoax"), plunged into the fluid bulk. The measurement accuracy is within ± 1°C.

2.3.3. The test section was equipped with three wall thermocouples close to the channel exit to record the crisis onset. Two resistance bridge devices were employed as burn-out detectors. The first device detected the resistance unbalance over the second half of the test element and the second monitored the outlet end. The unbalance signal was continuously recorded by a Leeds & Northrup potentiometer; the recorder itself actuated two microswitches (at both ends of the recording span). As burn out was approaching continuous hand adjustments were required, to counteract bridge unsettling and avoid spurions power trip. Microswitches were operated by the crisis thermocouple recorders to trip power as additional safety devices.

3. TEST ELEMENTS AND RANGE OF VARIABLES

3.1. The three tubular test sections, made of AISI 321 (EL G1) or AISI 316 (IT18 and IT22) stainless steel tubes of commercial type, cold-drawn without welding, had the same geometrical dimensions (Nom. I.D. 2.50 cm, heated length 240,160 and 80 cm), except for the inlet calming length (20 cm for EL G1, 120 cm for EL IT18 and IT22) and the wall thickness (2.5 mm for EL G1, 1.5 mm for EL IT18 and IT22).

EL G1, previously tested on the IETI-2 plant during the CAN-3 Program in 1963, was installed in Oct. 1966 on the IETI-3 plant for a preliminary check of the loop operation. A new test element (EL IT18) whose electrical resistance matched the d.c. generator was made for the tests at the SORIN facility caracteristics. A smaller wall thickness (1.5 mm) was adopted and improvements in the inlet section (calming length 120 cm) and instrumentation (immersed type inlet thermocouple) were introduced. Because of rather severe damage caused to EL IT18 by repeated burnouts, a new element (EL IT22, identical to EL IT18) was built for the experiments at the SORIN facility and for the latest ones at the IETI-3 plant.

Four power lugs allowed heating of different lengths (80, 160 and 240 cm): each copper lug, silver soldered to the tube, was also equipped with a pressure tap. Of all possible connections, three have been tested:

a) full heated length of 240 cm;
e) upstream heated span of 160 cm;
f) downstream heated span of 160 cm(+).

Dimensional parameters and adopted electrical connections are summarized in Table A, reporting also the plants where each element has been tested.

(+) No influence on the critical power value is expected from the difference in calming lengths between conn. e) and f) (see table 4), which are therefore considered identical. This assumption is well justified for negative inlet qualities.

3.2. The range of investigated variables is clearly shown in Table B. Only experiments under subcooled inlet conditions have been considered (positive inlet qualities are not obtainable at the SORIN facility).

Therefore only a few results from the Genoa IETI-2 plant, are available for comparison at the rated G values and $X_{in} < 0$.

4. EXPERIMENTAL PROCEDURE

4.1. Heat transfer crisis was reached by gradually increasing the test element power at constant flowrate, inlet quality and pressure, following the indications of the thermocouple(s), located 1 ÷ 3 cm upstream of the test section outlet, and at the same time the recording of the B.O. detector unbalance signal.

After getting one experimental point, the test element power was shut down, the inlet quality changed and a new experiment carried out.

As a general rule, the crisis was defined by the onset of temperature noise often preceded by a typical drop[5]. The B.O. detector signal recording(+) usually followed a similar path and the drop forewarning the crisis was in clear evidence (Fig. 20); the resistance unbalance signal was much faster than the thermocouple output and, under some circumstances, the detector tripped the power before any temperature peak could be observed. However in many a test, relatively "slow" crises were observed, typically at low inlet subcooling, and the power trip was often operated by hand before the intervention of the safety devices.

Much care was put in calibrating the B.O. detectors(°) in order to get almost the same sensitivity from the different devices employed by CISE and SORIN.

Experiments performed at SORIN with different adjustements of the B.O. detector threshold have proved that the effect on the critical power value does not exceed ≃ 1 ÷ 1.5%. The uncertainty due to the operator sensitivity at the power control desk should also be within this range.

(+) Almost always recorded for tests carried out with EL IT18 and IT22. For EL G1 no B.O. detector was employed during the test at the IETI-3 plant.

(°) And the temperature thresold above which power was automatically tripped at the SORIN plant.

4.2. The flowrate and pressure stability was generally satisfactory for the three plants at least for specific mass flowrates ≥ 110 g/cm^2s. At mass flowrates ≤ 80 g/cm^2s, i.e. at flowrates much lower than the values usually adopted on the three plants, pressure and flowrate control was sometimes critical, particularly at relatively strong subcooling.

When the inlet temperature approached the saturation value, inlet throttling was provided to avoid boiling in the flowrate measurement section upstream of the test element.

5. PRESENTATION OF RESULTS

5.1. All experimental data available from EL G1, at IETI-2 plant, can be found in ref. 3; only the experiments here considered are reported in appendix for easy reference; the results are listed as follows in tables 7 and 8:

- run No.
- total specific mass flowrate in the test element (G, g/cm^2s)
- absolute pressure at the test element outlet (P_o, kg/cm^2abs)
- pressure drop across the test element (ΔP, kg/cm^2)
- inlet and outlet qualities(+) by weight (X_{in}, X_o)
- critical power to the test element (W, kW)
- critical heat flux (∅, W/cm^2).

5.2. The raw experimental data from the IETI-3 plant (elements G1, IT18, IT22) have been worked out by means of a computer code for IBM 1800[6] and outputs are presented in tables 1 to 6. For this reason the number of digits reproduced in the tables does not correspond to the accuracy of the data.

The results given in tables 1 to 6 are listed as follows(°):

- name of test element and datum
- run No.
- total specific mass flowrate (G, g/cm^2s)
- inlet and outlet qualities(+), by weight (X_{in}, X_o)
- absolute pressure at inlet and outlet (P_{in}, P_o, kg/cm^2abs)
- critical power to the test element (W, kW)
- critical heat flux (∅, W/cm^2)

(+) Negative qualities correspond to subcooled water according to the following definition:

$$X = (H - H_{l,sat})/H_{gl}(P)$$

(°) The pressure drop across the test element was seldom measured and is never reported.

The symbol "x" at the left border means that the experiment is considered unreliable, i.e. affected by the spurious effects described in 6.1; brackets label the "spurious" points in Figs. 8 to 19; "OX" in Tables 1 to 6 means that small flowrate and pressure oscillations (up to ± 5% close to the crisis onset) were observed during the experiment considered.

5.3. The experimental data concerning the SORIN facility (EL IT22) are reported in Ref. 1: all experimental points are shown in Figs. 8 to 19 according to mass flowrate, pressure and heated length. Interpolation curves for all sets of data (+) are also plotted as well as a reference straight line corresponding to the critical power predicted by the CISE correlation (7), considered as reference value.

(+) Divided according to test elements and to the experimental facility, i.e. up to five different sources (see also Table C).

6.1. Reproducibility checks carried out with EL IT18 at the CISE IETI-3 plant (source 3 in table C) showed remarkable discrepancies between the experiments carried out in January 1967 and those of February 1967. The critical power data relevant to the latter are lower and more scattered than the former. Spurious phenomena associated with the hydraulic circuit were observed in carrying out these experiments: quite strong vibrations of the plant section connected with the test element; random onset of non-persistent red-hot spots in irregular positions along the test section at power levels much lower than the expected critical value, crisis recordings of the B.O. detector and thermocouples often different from the usual trend(+).

An inspection of the test element after ~ 1 month of experimental operation showed a thick incoherent layer of corrosion products (up to ~ 0.1 ÷ 0.5 mm) on the inner heat transfer surface: quite small solid particles in suspension fouled the circulating water.

Cleaning of the test section inner surface caused a transitory and slight improvement, and critical power values somewhat higher than before cleaning were obtained (compare runs relevant to 14th - 15th and to 16th Feb. 1967 in Table 4). The above spurious effects however appeared again, though the inner surface of EL IT18 was found clean and undamaged after a final inspection.

It was inferred that the accumulation of corrosion products from the circuit carbon steel is made of and the suspended solids fouling the water were responsible for the observed anomalous phenomena.

(+) The drop usually preceding the onset of the crisis is normally detected at the same time by the B.O. detector and by the thermocouple at the test section outlet, whereas for the above experiments the drop, if recorded, is detected only by one of the two devices (compare Fig. 20, run No 5 and No 25).

Therefore after carefully cleaning and pickling the whole hydraulic circuit, chemical treatment of the circulating water was provided (resin ion exchanger, hydrazine injection etc. as explained in 2.2.1). Experiments relevant to EL IT22, at the IETI-3 plant (source 5 in Table C), were carried out with clean water and spurious effects were no longer noticed: the relevant critical power values were found to be well reproducible and higher than the data from source 3.

6.2. Owing to the described experimental troubles, some of the data relevant to EL IT18 (source 3) are not to be considered reliable with respect to the results for EL IT22 (sources 4 and 5, SORIN and IETI-3 facilities).

For comparison's sake some experiments of source 3 have been discarded in Table C, according to the following criteria:

a) doubtful crisis onset recording (see footnote page 20)
b) severe experimental troubles, owing to the time integrated corrosion process, as described in 6.1.

The experiments not liable to be compared are labeled with the symbol "x" in Tables 1 to 6 and the corresponding points are bracketed in Figs. 8 to 19.

Also some experiments carried out with EL IT22 have not been taken into account in Table C, because of unstable flowrate and pressure conditions.

With these criteria a selection of "consistent data" has been made on the sets of the available experimental data (up to five sources).

6.3. The "consistent data" plotted in Figs. 8 to 19 in terms of critical power vs. negative inlet quality show a regular trend; each set of experimental points has been interpolated by a line with respect to which an average scattering has been tabulated (Table C), according to the following definition:

$$\sigma \% = \sqrt{\frac{1}{N} \Sigma \left(\frac{W_{exp} - \overline{W}}{\overline{W}}\right)^2} \cdot 100$$

where : N number of experimental points
W_{exp} measured critical power
$\bar{W}$ average power value from the interpolating line.

For all sources the scattering is limited to 1 ÷ 1.5%. CISE correlation(7) for critical power in uniformly heated round tubes was used to provide a reference standard for a quantitative comparison, and the deviation ε has been calculated for each experiment, according to the following formulae:

$$\varepsilon \% = \frac{W_{exp} - W_{calc}}{W_{calc}} \cdot 100$$

and averaging:

$$\bar{\varepsilon} = \frac{1}{N} \Sigma \varepsilon$$

where: $W_{calc} = \Gamma H_{gl} (a - X_{in}) \frac{L}{L+b}$

$$a = \frac{1-P/P_{cr}}{\sqrt[3]{G/100}} \qquad b = 0.315 \left(\frac{P_{cr}}{P} - 1\right)^{0.4} D^{1.4} G \text{ (CGS units)}$$

The average values of ε are reported, source by source, for each set of G,P,L in Table C. The "consistent" experimental data are plotted vs. predicted critical power(+) in Fig. 21, where a few points from Ref. 9 have also been added for comparison.

(+) For clarity's sake the magnitudes $W/\Gamma H_{gl}$ (= $X_o - X_{in}$, neglecting the pressure drop across the test section) are reported, so that points are arranged according to the mass flow-rate (low $W/\Gamma H_{gl}$, corresponding to high flowrate and viceversa).

6.4.1. The following remarks can be inferred from table C and from Fig. 21:

a) the critical power values of source 1 (IETI-2 plant) are the lowest and on the average by ~ 7.5% lower than the data of source 5: the maximum discrepancy amounts to some 10%.
b) The few experiments of source 2 (the first data obtained at the IETI-3 plant in Sept.-Oct. 1966) show the highest values of the critical power and agree within ~ 1 ÷ 1.5% with the data of source 5.
c) The critical power data of source 3, although cleared from "non consistent" experiments (see 6.2.), are on the average lower by ~ 5% than those from source 5. The discrepancy is higher than the average for some examples (Figs. 10,18,19), generally corresponding to the latest tests on EL IT18.
d) The discrepancy between sources 4 and 5, both corresponding to the most accurate experiments, is on the average ~ 3%; the data from source 5 are systematically higher than those from source 4, and the discrepancy grows with decreasing mass flowrate, pressure and inlet quality (up to 8 ÷ 10% at G = 80 and G = 110 g/cm^2s, P = 31 and 51 kg/cm^2a); at specific mass flowrate ≳ 220 g/cm^2s or at P = 61 kg/cm^2a. the discrepancy amounts to some 2 ÷ 4%.
e) In fig. 21 a few data relevant to a tubular test section (I.D. = 2.5. cm, L = 250 cm) and to a mass flowrate range slightly overlapping with ours (G = 40 ÷ 100 g/cm^2s) are reported from Becker[9] ; Becker's points at 51 kg/cm^2a. lie somewhat 1-2% below CISE correlation. Therefore they do not agree satisfactorily with sources 4 and 5, since the relevant data at G = 40 ÷ 80 g/cm^2s are underpredicted by the correlation by ~ 2% and by 10% for sources 4 and 5 respectively. Other data concerning the same test section dimensions for a direct comparison have not been found in the literature.

6.4.2. The agreement between sources 2 and 5 and the discrepancy between sources 3 and 5, all of them relevant to the IETI-3 plant, may be explained taking into account water purity effects; the experiments of source 2 were carried out when the plant components more involved in the corrosion process (typically the degassifier) were still new and clean; the experiments of source 3 were carried out after some time of plant operation during which the water was getting more and more fouled by corrosion and erosion particles: after the chemical treatment, water purity was assured and the experiments of source 5 agreed with those of source 2(+).

The average difference between the data from sources 4 and 5 (the latter being on the average by 3% higher than the former) can be considered as satisfactory, if the differences between the hydraulic circuit schemes of the two plants, the measuring devices and the operating staffs is taken into account; but there are relatively high and systematical discrepancies (up to 8-10%) at low mass flowrate(°) and at low pressure(").

It has been suggested that the discrepancy between sources 4 and 5 may be justified with the different "response" of the two circuits to decreasing flowrate, pressure and inlet quality, which are destabilizing factors, as it is well known from the experimental operation of two-phase plants. However no appreciable unstable flow conditions were detected by manometers and flowrate measuring devices for the experiments considered.

(+) The slight discrepancy between sources 2 and 5 might be attributed either to the different wall thickness of the test sections (s = 2.5 mm for EL G1 (source 2) and s = 1.5 mm for EL IT22 (source 5)), or to the crisis detecting devices (for the experiments of source 2 no B.O. detector was employed).

(°) The parameter to be considered may be the total mass flowrate instead of the specific mass flowrate in the test section, but this topic can not be investigated on account of the present results relevant to one diameter and cross section only.

(") Only minor differences in the trends of critical power vs. inlet quality curves are observed: there is a general tendency for the discrepancy to decrease at low subcooling for $G \leq 110$ g/cm^{2}s and the opposite tendency (vanishing dicrepancy at high subcooling) for $G > 220$ g/cm^{2}s.

A perusal of experimental recordings assures that the crisis onset corresponds to the usual phenomenological trend. The following recordings are reported for example in Figs. 22 - 24:

a) Fig. 22	G = 110 g/cm^{2}s	P_o = 31 kg/cm^{2}a	X_{in} = - 0.20	sources	3-4-5
b) Fig. 23	G = 110 "	P_o = 51 "	X_{in} = - 0.20	"	"
c) Fig. 24	G = 300 "	P_o = 51 "	X_{in} = - 0.20	"	"

No useful suggestion can be inferred either from the comparison between recordings, relevant to the same inlet conditions but to different sources, or from the comparison between a) or b), corresponding to a strong discrepancy between different sources, and c), corresponding to a good agreement.

Disturbance effects, different from plant to plant, may be hypothetically taken into consideration:

- at the IETI-3 plant, water was fed to the test element through a mixer (usually employed for two-phase inlet), whereas at the SORIN facility, water enters the test element directly downstream of the turbine flow meter, but the disturbance is unlikely to be effective up to ~ 40 ÷ 50 diameters from the inlet (calming length) in subcooled water.
- A backstream effect of the outlet configuration might be tentatively invoked in the comparison between SORIN and IETI-3 facilities, since in the former case the by-pass subcooled water flowrate (see Figs. 3 and 7) was mixed with the steam-water mixture leaving the test section just downstream of the outlet end of the heated channel, while in the latter a long piping connected the test section with a separator.
- Strong and noisy vibrations (not necessarily involving flow instability) were often observed at power levels some 30 - 50% lower than the critical value particularly at low G and X_{in} at the IETI-3 plant. The phenomenon faded away with power increase and tended to vanish near the crisis. It is obscure whether it can have a particular meaning and whether the mechanical vibrations of the loop section connected with the test element may somehow affect the crisis onset.

Therefore the influence of unknown or uncertain parameters or plant components should be admitted in order to account for the experimental discrepancy between results from sources 4 and 5 (the discrepancy is however limited to the range $G \lesssim 110\ g/cm^2s$, $P \leq 51\ kg/cm^2a$). A strong discrepancy can be observed between sources 1 and 5[(+)] (the power values from source 5 being systematically higher by about 8-10% than those from source 1) and between source 5 and the data from ref. 9 (Fig. 21); neither for these examples have a satisfactory explanation or suggestion been found.

6.5.1. A similar discrepancy (up to ~ 10%) (Fig. 25) between experiments carried out with the same test element on different rigs has been found by Lee[(10)], who compares the data concerning tubular test sections (I.D. = 0.9 ÷ 1.2 cm, L = 85 ÷ 300 cm) at P 70 kg/cm^2abs, G = 135 ÷ 270 g/cm^2s, subcooled inlet. Again there is a relatively strong discrepancy at low flowrates while data from different rigs tend to agree satisfactorily at high flowrates. The experiments were carried out at one pressure and it is not possible to investigate the effect of this parameter from Lee's data.

Just like in our case, no evident explanation has been found by Lee to justify the observed discrepancies and no component or device of the plants considered has been supposed to be particularly responsible for the systematic and relatively strong effect focused by the comparison.

(+) The equation of water purity might be suggested to explain partially the strong discrepancy (~ 7.5%) between source 1 and 5, since at the IETI-2 plant, whose hydraulic circuit was quite similar to IETI-3, water chemistry was not so carefully accounted for as at the IETI-3 plant (source 5), the data from the IETI-2 plant are however well reproducible and no phenomena were observed like the spurious effects, noted during the commissioning of the IETI-3 plant (see 6.1., source 3). Therefore water chemical impurity is unlikely to have so sensibly affected the critical power value.

A survey of literature data from different sources (Fig. 26)[(+)] (tubular geometry, $D \simeq 0.92 \div 1.05$ cm, $L \cong 80 - 250$ cm, P = 70 and $P \cong 40 \div 50$ kg/cm^2) seems to confirm the above described tendency: relatively good agreement at high mass flowrate and $P = 60 \div 70$ kg/cm^2 and stratification at low mass flowrate and at low pressure.

According to a rough estimate of the stratification in the plot of Fig. 26, the maximum scattering of all points ranges from $\pm$ 10% to $\pm$ 15%, while data from individual sources are scattered by about $\pm 3 \div 6$%. Also the trends of average curves differ from source to source; for instance the interpolating curve of AEEW data (see also Fig. 25) shows a typical swerve when the mass flowrate changes from G = 135 g/cm^{2}s to G = 100 g/cm^{2}s, which does not occur for other sources (compare Becker's and CISE data with AEEW and Columbia University data at P = 70 kg/cm^2).

Of course it must be kept in mind that the reduction by CISE correlation of the data relevant to near, but different conditions introduces additional scattering, which overlaps with the actual effect to be evidenced.

6.5.2. Experiments summarized in Figs. 21 and 25 carried out in identical or similar conditions, can be better compared. It is to be observed that UKAEA data (Fig. 25) considered source by source (i.e. rig by rig), are more scattered than those from the present report (Fig. 21), since in the former case points relevant to different test sections have been put together[(°)] and the sets of data of Fig. 25 are almost twice as many

(+) The experimental data, reported in Fig. 26, are plotted vs. the predicted value, according to CISE correlation[(7)]. It takes well into account the effects of heated length and inlet quality, but it tends to underestimate the critical power value at low G and low P. Such correlation has been used however only to provide a useful reference standard for comparison's sake.

(°) The cross section diameter ranges from 0.952 to 1.18 cm, the heated length from 86 to 305 cm; however from Fig. 26 it can be inferred that the stratification due to different geometrical dimensions can be neglected in first approximation, its only effect being to increase the scattering of each source around its average curve.

as those of Fig. 21.

To better evidence the discrepancy between different sources, experimental points have been subdivided according to the deviation from CISE correlation[7], (and, if necessary to flowrate groups[+]) and frequencies have been plotted in histograms. The two comprehensive histograms have been interpolated by normal distributions: the root mean square error appears to be greater, as expected for UKAEA data (σ = 5.93%) as to those presented in this report (σ = 4.75%). At any rate an order of magnitude of the standard deviation ($\sigma = 5 \div 6\%$) has been obtained.

To better emphasize the influence of the experimental rig three sources have been selected both from Fig. 27 (1, 4 and 5) and Fig. 28 (1 MW ICL AERE data at $G \gtrsim 140\ g/cm^2s$ only), and the partial histograms have been modified to normalize their areas to be same value: therefore in Fig. 29 each source (i.e. each rig) has been given the same statistical weight.

The standard deviations reported in Figs. 27 and 28 show a slight tendency to approach each other (4.95% and 5.8% - Fig. 29) and the average discrepancy between different sources is at once apparent.

[+] As the deviation from the predicted value strongly increases with decreasing flowrate for UKAEA data, the histograms of Fig. 28 have been centered around the mean deviation $\bar{\varepsilon}_G$, pertinent to each flow rate group and averaged over the three sources. The average deviation of data in Fig. 21 has been considered as independent of flow rate.

7. CONCLUSIONS

The following conclusions can be drawn from this investigation:

- The critical power values which can be measured with the same tubular test element but with different experimental facilities generally show a satisfactory agreement (i.e. within the foreseen measurement inaccuracy) but in some cases noticeable discrepancies may arise (even up to 10 ÷ 12%).
- If a comparison is made between data relevant to different tubular test elements (but having the same dimensions) as well as to different experimental facilities, the reproducibility is (for the case investigated):

  standard deviation ± 5%

  maximum deviation ± 11.2%
- The same comparison, taking however into account data relevant to tubes having different lengths, gives the following results:

  standard deviation ± 5.8%

  maximum deviation ± 15%

  These higher values are also due to the increased number of sets of UKAEA data.
- The observed deviations are noticeably larger than the measurement inaccuracy, thus indicating the presence of an additional effect on heat transfer crisis; moreover the various attempts to identify it have been so far unuccessful and further systematic investigations should be carried out to obtain a clarifying picture.
- As for the rod bundle geometry, a further effect which is related to the particular test element building must be taken into account; no data have been collected on this subject during the present investigation, but experiments carried out at Winfrith by UKAEA(19) suggest that a significant scatter may exist (± 6%).
- The margin of uncertainty affecting critical power data have several pratical consequences of which the main ones are:

a) for any correlation derived for predicting critical power values, there is a minimum band of uncertainty which is larger than the one due to measurement errors, and which, for tubular elements, can be evaluated at approximately $\pm$ 15% (6% standard deviation). In the case of rod bundles this figures increases but the amount cannot even approximately be established.

b) Any limited set of data, relevant to given power channel, cannot be used for predicting critical power data (for example in a reactor power channel), without taking into account an uncertainty band amounting at least to $\pm$ 15% (6% standard deviation). In particular full scale out of pile experiments are significant only if taking into account such uncertainties.

- Fouling due to water impurities (in particular to the presence of iron oxides) may have even an appreciable effect on burnout. Also careful water chemistry control is important in obtaining reproducible data. These factors sensibly affect boiling heat transfer[20]. No systematic investigation has been carried out as for their impact on critical power; an order of magnitude may be however inferred from the data of source 3 (fouled water), whose critical power is lower by some 5 ÷ 20% than those of source 5 (clean water).

Acknowledgements

The authors wish to thank Messrs. A. Campanile, G. Galimi and M. Goffi of SORIN for carrying out the experiments with the SORIN high pressure facility and for giving a valuable contribution to the discussion of the results.

Particular thanks are also due to Mr. G.P. Gaspari for his helpful criticism.

The contribution of all those who cooperated in setting up the test assemblies (in particular of Mr. G.F. Germani) and in carrying out the experimental program (in particular of Messrs. V. Tarzia and P. Casazza) is gratefully acknowledged. The authors are also grateful to ENEL and to the staff of the Emilia thermoelectric power station in Piacenza for their assistance and cooperation.

Nomenclature

Roman letters

D	diameter	cm
G	specific mass flowrate	g/cm^2s
H	specific enthalpy	kcal/kg
H_{gl}	heat of vaporization	kcal/kg
L	heated length	cm
L_{pt}	pressure taps distance	cm
P	absolute pressure	kg/cm^2abs
P_{cr}	critical pressure	kg/cm^2abs
W	critical power	kW
$\bar{W}$	average critical power	kW
X	quality (by weight $= \frac{H-H_{l,sat}}{H_{gl}}$)	

Greek letters

ε	deviation of measured from predicted critical power	%
$\bar{\varepsilon}_G$	deviation average for a constant G	%
Γ	mass flowrate	kg/h
ΔP	pressure drop	kg/cm^2
σ	standard deviation	%
ϕ	heat flux	W/cm^2

Subscripts

calc	calculated
cr	critical
exp	experimental
in	inlet
l	liquid phase
o	outlet
sat	saturation

References

1. A. Campanile, G. Galimi, M. Goffi: "Critical power experiments conducted with a closed circuit facility on the IT22 test section cooled by steam-water mixture" - SORIN Report T/516 (1967).
2. N. Adorni, A. Alessandrini, G. Peterlongo, R. Ravetta: "Large scale experiments on heat transfer and hydrodinamics with steam-water mixtures: Description of the experimental plant". CISE Report R-79 (1963).
3. A. Alessandrini, G. Peterlongo, R. Ravetta: " Critical heat flux and pressure drop measurements in round vertical tubes at the pressure of 51 kg/cm^2abs". CISE Report R-86.
4. Annual Report of the CIRENE-3 Program 1965. CISE, Milan, Jan. 1966.
5. S. Bertoletti, C. Lombardi, M. Silvestri: "Heat transfer to steam--water mixtures" CISE Report R-78 (1964).
6. G.P. Gaspari, A. Milani: "Codice Resegone per l'elaborazione delle letture strumentali ottenute sugli impianti IETI-1 e IETI-3 e sottoprogrammi per il calcolo delle proprietà fisiche dell'acqua e del vapore". CISE R-235 (1967).
7. S. Bertoletti, G.P. Gaspari, C. Lombardi, G. Peterlongo, M. Silvestri, F.A Tacconi: "Heat transfer crisis with steam-water mixtures". Energia Nucleare 12, 3, 121 (1965).
8. F. Biancone, A. Campanile, G. Galimi, M. Goffi: "Forced convection burnout and hydrodynamic instability experiments for water at high pressure - Part I". SORIN - EUR 2490/e (1965).
9. K.M. Becker: "An analytical and experimental study of burnout conditions in vertical round ducts". AE-RTL 778 - Studsvik (1965).
10. D.H. Lee: "An experimental investigation of forced convection burnout in high pressure water - Part III". AEEW R 355 - Winfrith 1965.
11. D.H. Lee, J.D. Obertelli: "An experimental investigation of forced convection burnout in high pressure water - Part. I". AEEW R 213 - Winfrith 1963.
12. S. Bertoletti, G.P. Gaspari, C. Lombardi, G. Soldaini, R. Zavattarelli: "Heat transfer crisis in steam-water mixture. Experimental data in round tubes and vertical upflow obtained during the CAN-2 program". CISE Report R-90 (1964).

13. B. Matzner, J.E. Casterline, E.O. Moeck, G.A. Wikhammer: "Critical heat flux in long tubes at 1000 psi with and without swirl promoters". ASME 65 WA/HT 30 (1965).
14. V.N. Smolin, V.K. Poliakov, V.I. Yesikov: "On the heat transfer crisis in a steam-generating tube" Atom. Energija, Oct. 1962.
15. United Kingdom Atomic Energy Authority: "European Two Phase Heat Transfer Meeting". Durley Hall, Bournemouth - June 1967.
16. R.V. Macbeth: "Burnout analysis - Part. 5: examination of published world data for rod bundles". AEEW - R 358 (1964).
17. P.G. Barnett: "A correlation of burnout data for uniformly heated annuli and its use for predicting burnout in uniformly heated rod bundles". AEEW - R 463 (1966).
18. K.M. Becker: "A correlation for burnout predictions in vertical rod bundles" - S-349. Paper presented at the Symposium on Boiling Crisis in Two-Phase Flow - Ispra, June 1966.
19. G.F. Stevens, R.W. Wood: "A comparison between burnout data for 19 rod cluster test sections cooled by freon-12 at 155 lb/in^2(abs) and by water at 1000 psi in vertical upflow". AEEW - R 468 (1966).
20. W.C. Elrod, J.A. Clark, E.R. Lady, H. Herte: "Boiling heat-transfer data at low heat flux". ASME Journal of Heat Transfer - Aug. 1967, 235 - 243.

TABLE A — TEST ELEMENTS

Round Tubes — Uniform Heat Flux — Vertical upflow

ELEMENT connection	I. D. internal diameter (cm)	O. D. outer diameter (cm)	L heated length (cm)	L_{pt} press.taps distance (cm)	S heated area (cm^2)	$L_{c,s}$ calming length (cm)	EXPERIMENTAL PLANT
G1/a	2.49	3.00	239.0	248.8	1870	~ 20	CISE-IETI 2 - Genova
G1/e			159.0	164.0	1245	~ 20	CISE-IETI 3 - Piacenza
IT18/a	2.51	2.81	239.0	248.0	1886	~ 20	CISE-IETI 3 - Piacenza
IT18/e			159.2	165.2	1255	~ 120	
IT22/a	2.50	2.82	239.1	246.6	1883	~ 105	SORIN PLANT-Saluggia
IT22/f			159.3	165	1255	~ 185	CISE-IETI 3 - Piacenza

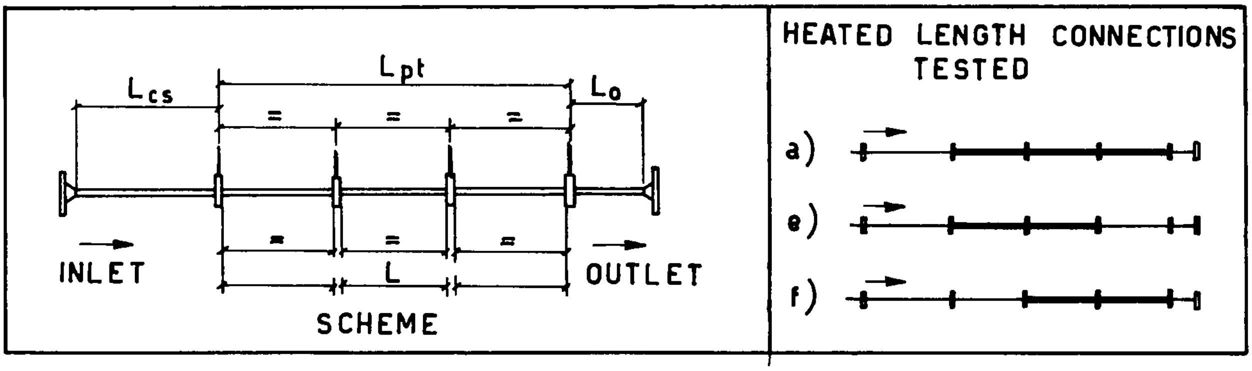

TABLE B - RANGE OF EXPERIMENTAL DATA

REFERENCE	TABLE N.	ELEMENT connection	P_o outlet pressure (kg/cm^2 a)	G Specific mass flowrate (g/cm^2 s)	X_{in} inlet quality (by weight)	X_o outlet quality (by weight)	ϕ heat flux (W/cm^2)
PRESENT REPORT	1	G1-a	51	110; 220; 380	- 0.25 ÷ 0	+.04 ÷ .5	190÷300
	2	G1-e	51	220	-.20 ÷ 0	+.05 ÷ .5	270 ÷ 325
	3	IT18-a	51 31 ; 61	40; 80; 110; 220; 300; 380 110; 220	-.25 ÷ 0	0 ÷ +.84	145 ÷ 330
	4	IT18-e	51	220; 300	-.17 ÷ .0	0 ÷ +.18	222 ÷ 330
	5	IT22-a	51 31 ; 61	40; 80; 110; 220; 300; 380 110; 220	-.28 ÷ .0	0 ÷ +.83	143 ÷ 320
	6	IT22-f	51	220; 300	-.19 ÷ 0	0 ÷ +.16	265 ÷ 343
REF (3)	7	G1-a	51	110; 220; 300; 380	-.20 ÷ -0.1	0 ÷ 0.38	213 ÷ 320
	8	G1-f	51	220; 300	-.20 ÷ -.1	0 ÷ 0.10	260 ÷ 340
REF (1)	-	IT22-a	51 31; 61	40; 110; 220; 300; 380 110; 220	-.30 ÷ 0	0 ÷ .85	140 ÷ 320
	-	IT22-f	51	220; 300	-.20 ÷ 0	0 ÷ .15	260 ÷ 340

TABLE C

				SOURCE 1 (∇)			SOURCE 2 (▲)			SOURCE 3 (●)			SOURCE 4 (○)			SOURCE 5 (x)		
FIG. No.	L	P	G	ELG1-IETI 2			ELG1-IETI 3			IT18-IETI 3			IT22-SORIN			IT22-IETI 3		
	cm	kg/cm² a	g/cm² s	N.	σ %	ε %	N.	σ %	ε %	N.	σ %	ε %	N.	σ %	ε %	N.	σ %	ε %
8	240	51	40							5	1.4	+ 3.6	10	2.0	− 0.5	2	2.0	+ 4.3
9			80							7	0.7	+ 8.6	7	0.9	+ 5.2	6	2.0	+ 11.1
10			110	6	0.8	+ 1.3	8	1.4	+ 9.5	9	1.1	+ 2.9	7	0.7	+ 2.3	7	1.1	+ 8.5
11			220	6	0.3	− 4.1	5	0.3	+ 6.8	6	1.1	+ 1.1	6	0.6	+ 2.3	8	0.9	+ 6.0
12			300	6	1.4	− 4.0				6	0.8	− 0.9	8	1.0	+ 2.6	6	0.5	+ 3.7
13			380	6	0.5	+ 2.1	3	1.4	+ 9.8				6	1.3	+ 3.2	5	1.2	+ 7.6
G-averaged errors :				24	~0.8	− 1.2	16	~1.2	+ 8.7	33	~ 1.0	13.2	44	~1.2	+ 2.3	34	~1.3	+ 7.15
14	240	31	110							4	1.2	+ 8.4	8	0.8	+ 5.7	6	1.5	+ 14.5
15			220										5	0.2	+ 17.5	4	0.6	+ 21.7
16		61	110							4	0.6	+ 0.3	9	1.2	+ 2.6	4	0.6	+ 3.3
17			220							5	0.9	− 4.8	9	1.1	− 4.5	6	1.0	− 1.0
18	160	51	220	6	0.9	− 3.2	3	0.7	+ 6.1	17	2.1	− 0.4	10	1.7	+ 3.6	5	0.3	+ 6.15
19			300	5	0.9	+ 1.5				10	0. 8	+ 0.1	6	1.6	+ 3.7	6	0.9	+ 7.5
Total average errors				35	~0.9	− 1.2	19	~1.1	+ 7.6	73	~1.4	+ 1.5	91	~1.2	+ 3.0	65	~1.1	+ 6.3

CRITICAL POWER - IETI 3...PLANT - EL.G1-a. TABLE 1....

REMARKS	RUN.	No.	G	X_{in}	X_e	P_{in}	P_o	W	ϕ
			$g/cm^2 s$	by weight		kg/cm^2 abs		kW	W/cm^2
G1	17/10/66	8	118.29	-0.141	0.359	51.5	51.1	471.9	252.3
G1	18/10/66	8	108.16	-0.125	0.407	51.3	50.9	459.2	245.5
G1	19/10/66	10	106.90	-0.052	0.444	51.3	51.0	423.5	226.5
G1	19/10/66	11	111.51	-0.096	0.404	52.4	52.1	443.0	236.9
G1	19/10/66	12	109.07	-0.128	0.390	52.2	51.9	449.5	240.3
G1	19/10/66	13	109.07	-0.124	0.392	51.4	51.1	448.8	240.0
G1	19/10/66	14	108.16	-0.167	0.367	51.1	50.8	461.0	246.5
G1	19/10/66	15	108.60	-0.220	0.349	51.4	51.1	492.9	263.5
G1	20/10/66	25	217.85	-0.056	0.210	51.4	50.8	460.3	246.1
G1	20/10/66	26	214.26	-0.118	0.170	51.5	51.0	490.9	262.5
G1	20/10/66	27	217.89	-0.254	0.076	51.8	51.1	570.5	305.1
G1	7/10/66	9	217.27	-0.049	0.214	51.9	51.2	452.7	242.0
G1	7/10/66	10	219.84	-0.109	0.170	50.9	50.3	488.2	261.0
G1	13/10/66	7	379.68	-0.042	0.110	51.7	51.0	456.4	244.0
G1	21/10/66	34	379.17	-0.096	0.066	51.9	51.0	483.5	258.6
G1	21/10/66	35	379.09	-0.148	0.039	52.0	51.3	559.4	299.1

CRITICAL POWER - IETI 3...PLANT - EL.G1-e. TABLE 2....

REMARKS	RUN.	No.	G	X_{in}	X_e	P_{in}	P_o	W	ϕ
			$g/cm^2 s$	by weight		kg/cm^2 abs		kW	W/cm^2
G1	19/10/66	17	216.23	-0.184	0.054	51.2	50.0	404.6	325.0
G1	19/10/66	18	216.82	-0.095	0.111	51.1	50.8	355.6	285.7
G1	19/10/66	19	216.77	-0.046	0.153	51.1	50.8	343.7	276.1

CRITICAL POWER - IETI 3...PLANT - EL.IT18-a TABLE 3....

REMARKS	RUN.	No.	G	X_{in}	X_e	P_{in}	P_o	W	ϕ
			$g/cm^2 s$	by weight		kg/cm^2 abs		kW	W/cm^2
IT18	20/1/67	18	39.69	-0.197	0.798	51.2	51.0	321.0	170.2
IT18	20/1/67	19	39.54	-0.129	0.818	51.5	51.3	303.8	161.1
IT18	20/1/67	20	36.93	-0.076	0.838	51.2	51.0	274.3	145.4
IT18	20/1/67	21	39.97	-0.059	0.792	51.4	51.1	276.2	146.4
IT18	20/1/67	22	40.16	-0.284	0.777	50.9	50.6	346.9	183.9
IT18	19/1/67	10	75.94	-0.257	0.489	50.9	50.5	460.6	244.2
IT18	19/1/67	12	77.92	-0.161	0.519	51.7	51.2	429.7	227.8
IT18	20/1/67	13	87.32	-0.095	0.484	51.6	51.2	410.3	217.5
IT18	20/1/67	14	82.08	-0.081	0.522	52.4	52.0	400.3	212.2
IT18	20/1/67	15	80.48	-0.072	0.532	51.9	51.5	393.9	208.8
IT18	20/1/67	16	83.27	-0.028	0.534	51.2	50.9	380.7	201.8
IT18	20/1/67	17	79.85	-0.222	0.466	51.4	51.0	446.3	236.6
IT18	24/1/67	43	110.08	-0.211	0.320	30.4	30.0	522.6	277.1
IT18	24/1/67	44	111.35	-0.150	0.363	31.6	31.0	506.2	268.4
IT18	24/1/67	45	109.51	-0.089	0.397	31.2	30.5	472.8	250.6
IT18	24/1/67	46	111.21	-0.041	0.405	32.4	31.8	438.8	232.6
IT18	25/1/67	47	110.67	-0.183	0.318	61.8	61.2	430.1	228.0
IT18	25/1/67	48	108.20	-0.149	0.337	61.8	61.2	407.6	216.1
IT18	25/1/67	49	108.17	-0.082	0.369	61.6	61.1	379.5	201.2
IT18	25/1/67	50	108.55	-0.049	0.375	62.2	61.8	356.6	189.1

CRITICAL POWER - IETI 3...PLANT - ELIT18-a TABLE 3(cont)

REMARKS - RUN. No.			G	X_{in}	X_e	P_{in}	P_e	W	ϕ
			g/cm² s	by weight		kg/cm² abs		kW	W/cm²
	IT18 20/1/67	23	108.10	-0.255	0.302	52.2	50.8	484.9	257.1
	IT18 20/1/67	24	113.92	-0.181	0.321	52.2	51.8	462.1	245.0
	IT18 20/1/67	25	108.85	-0.176	0.339	51.4	51.0	454.7	241.1
	IT18 20/1/67	26	108.20	-0.098	0.378	52.0	51.6	416.8	221.0
	IT18 13/1/67	3	108.55	-0.100	0.375	50.6	50.1	419.9	222.6
	IT18 16/1/67	4	113.63	-0.271	0.264	51.5	51.2	493.6	261.7
x	IT18 16/1/67	5	107.70	-0.182	0.322	51.3	51.0	441.5	234.1
x	IT18 16/1/67	6	112.48	-0.084	0.350	51.3	51.0	396.2	210.1
	IT18 18/1/67	7	109.47	-0.232	0.309	51.2	50.9	480.5	254.8
	IT18 18/1/67	8	110.19	-0.197	0.334	51.4	51.0	475.1	251.9
	IT18 18/1/67	9	108.17	-0.131	0.373	51.1	50.7	443.5	235.1
x	IT18 10/2/67	82	107.45	-0.060	0.427	51.5	51.0	424.6	225.1
x	IT18 10/2/67	83	112.35	-0.159	0.309	51.7	51.2	426.1	225.9
x	IT18 10/2/67	84	108.59	-0.198	0.301	51.8	51.3	438.5	232.5
	IT18 24/1/67	38	221.86	-0.201	0.072	61.7	61.2	470.6	249.5
	IT18 24/1/67	39	218.88	-0.155	0.107	61.4	61.0	446.6	236.8
	IT18 24/1/67	40	218.39	-0.090	0.150	61.4	61.0	406.2	215.3
	IT18 24/1/67	41	219.75	-0.052	0.181	61.9	61.2	397.2	210.6
	IT18 24/1/67	42	223.07	-0.029	0.195	62.2	61.5	385.1	204.1
	IT18 12/1/67	1	214.57	-0.123	0.150	51.4	51.0	474.1	251.4
	IT18 12/1/67	2	215.52	-0.077	0.178	51.4	51.0	445.8	236.3
	IT18 23/1/67	27	214.13	-0.164	0.119	51.5	51.0	492.0	260.9
	IT18 23/1/67	28	218.88	-0.117	0.149	51.7	51.1	469.6	249.0
	IT18 23/1/67	29	215.64	-0.078	0.179	51.6	51.0	448.0	237.5
	IT18 23/1/67	30	217.46	-0.047	0.198	51.5	51.0	431.9	229.0
	IT18 23/1/67	31	297.74	-0.183	0.028	51.8	51.2	507.0	268.8
	IT18 23/1/67	32	298.39	-0.109	0.081	51.7	51.1	456.3	241.9
	IT18 23/1/67	33	296.15	-0.048	0.137	52.2	51.5	439.5	233.0
	IT18 23/1/67	34	290.32	-0.017	0.165	52.2	51.2	423.3	224.4
	IT18 23/1/67	35	299.03	-0.124	0.067	51.7	51.1	460.6	244.2
	IT18 23/1/67	36	298.90	-0.175	0.028	51.2	50.8	492.4	261.1
x	IT18 8/2/67	67	298.66	-0.088	0.089	52.1	51.2	423.1	224.3
x	IT18 8/2/67	68	296.51	-0.099	0.076	52.1	51.2	415.9	220.5
x	IT18 8/2/67	69	292.88	-0.078	0.100	52.1	51.2	415.9	220.5
x	IT18 9/2/67	70	297.97	-0.142	0.050	51.7	51.0	459.6	243.7
x	IT18 9/2/67	71	297.55	-0.198	0.022	51.7	51.0	526.4	279.1
x	IT18 10/2/67	76	293.58	-0.083	0.098	51.6	51.0	427.4	226.6
x	IT18 10/2/67	77	292.87	-0.028	0.148	51.8	51.0	415.6	220.3
x	IT18 10/2/67	79	300.24	-0.054	0.116	51.7	51.0	409.6	217.2
x	IT18 10/2/67	80	304.96	-0.071	0.098	52.1	51.3	413.6	219.3
x	IT18 8/2/67	60	375.66	-0.096	0.048	51.9	51.0	432.5	229.3
x	IT18 8/2/67	61	373.30	-0.031	0.111	51.9	51.0	424.0	224.8
x	IT18 8/2/67	62	380.04	-0.189	-0.009	51.8	51.0	546.7	289.9
x	IT18 8/2/67	63	385.75	-0.194	-0.014	52.8	52.0	549.3	291.2
x	IT18 8/2/67	64	376.08	-0.153	0.005	51.8	51.0	474.1	251.4
x	IT18 8/2/67	65	370.71	-0.050	0.088	51.7	50.8	409.9	217.3
x	IT18 8/2/67	66	377.40	-0.026	0.113	52.3	51.0	415.5	220.3
x	IT18 9/2/67	72	216.51	-0.130	0.133	51.3	50.8	461.7	244.8
x	IT18 9/2/67	73	214.45	-0.068	0.176	51.7	51.0	423.1	224.3
x	IT18 9/2/67	74	216.83	-0.076	0.168	51.9	51.2	426.7	226.2
x	IT18 9/2/67	75	222.06	-0.053	0.180	51.7	51.0	417.5	221.3
x	IT18 10/2/67	78	220.33	-0.050	0.185	51.7	51.0	419.1	222.2
x	IT18 10/2/67	81	224.28	-0.053	0.178	51.8	51.1	418.0	221.6

CRITICAL POWER - IETI.3...PLANT - ELIT18-e TABLE 4....

REMARKS	RUN. No.	G	X_{in}	X_e	P_{in}	P_o	W	ϕ
		$g/cm^2 s$	by weight		kg/cm^2 abs		kW	W/cm^2
x	IT18 14/2/67 85	218.21	-0.098	0.075	51.4	51.0	305.7	243.6
x	IT18 14/2/67 86	216.88	-0.135	0.052	51.4	51.0	327.9	261.3
x	IT18 14/2/67 87	216.02	-0.227	0.005	51.4	51.0	405.2	322.9
x	IT18 15/2/67 99	219.21	-0.022	0.136	52.3	51.8	278.6	222.0
x	IT18 15/2/67100	218.42	-0.018	0.153	51.2	50.7	302.6	241.1
x	IT18 15/2/67101	223.82	-0.015	0.155	51.5	51.0	307.0	244.6
x	IT18 15/2/67102	221.07	-0.076	0.106	52.1	51.5	324.4	258.5
x	IT18 15/2/67 88	297.79	-0.050	0.067	51.7	51.0	279.9	223.0
x	IT18 15/2/67 89	295.75	-0.028	0.095	51.7	51.0	291.8	232.5
x	IT18 15/2/67 90	293.40	-0.024	0.101	51.7	51.0	295.0	235.1
x	IT18 15/2/67 91	300.24	-0.054	0.064	51.7	51.0	284.0	226.3
x	IT18 15/2/67 92	300.92	-0.055	0.062	51.7	51.0	281.8	224.5
x	IT18 15/2/67 93	304.81	-0.113	0.024	51.5	51.0	336.8	268.3
x	IT18 15/2/67 94	297.97	-0.142	0.010	51.5	51.0	365.1	290.9
x	IT18 15/2/67 95	295.86	-0.091	0.038	51.5	51.0	307.5	245.0
x	IT18 15/2/67 96	296.46	-0.178	-0.005	51.5	51.0	411.6	327.9
x	IT18 15/2/67 97	297.09	-0.031	0.093	51.7	51.0	296.2	236.0
x	IT18 15/2/67 98	299.56	-0.053	0.066	51.5	50.9	287.4	229.0
(*)	IT18 16/2/67103	221.73	-0.063	0.126	51.5	51.0	338.6	269.8
	IT18 16/2/67104	219.39	-0.058	0.133	51.4	50.9	338.1	269.4
	IT18 16/2/67105	219.43	-0.011	0.164	51.4	52.0	315.9	251.7
	IT18 16/2/67106	220.76	-0.025	0.155	51.6	51.0	321.3	256.0
	IT18 16/2/67107	221.68	-0.118	0.074	51.5	51.0	344.0	274.1
	IT18 16/2/67108	225.83	-0.123	0.065	51.5	51.0	344.0	274.1
	IT18 16/2/67109	223.02	-0.203	0.022	51.5	51.0	406.7	324.1
	IT18 16/2/67110	222.27	-0.156	0.046	51.5	51.0	363.7	289.8
	IT18 17/2/67111	216.42	-0.102	0.089	51.3	50.8	334.3	266.3
	IT18 17/2/67112	224.41	-0.167	0.041	51.5	51.0	377.9	301.1
	IT18 17/2/67113	225.01	-0.142	0.053	51.5	51.0	354.2	282.2
	IT18 20/2/67120	217.88	-0.037	0.143	51.5	51.0	317.0	252.5
	IT18 20/2/67121	216.92	0.001	0.176	51.6	51.0	305.5	243.4
	IT18 20/2/67122	219.39	-0.059	0.121	51.5	51.0	319.5	254.6
	IT18 20/2/67127	224.88	-0.136	0.056	51.5	51.0	348.1	277.3
	IT18 20/2/67128	215.01	-0.029	0.152	51.0	50.5	314.4	250.5
	IT18 20/2/67129	222.33	-0.129	0.061	51.1	50.6	342.7	273.1
	IT18 17/2/67114	301.69	-0.122	0.026	51.4	50.8	359.6	286.5
	IT18 17/2/67115	298.65	-0.173	-0.000	51.6	51.0	412.7	328.8
	IT18 17/2/67116	297.13	-0.138	0.017	51.6	51.0	371.3	295.9
	IT18 17/2/67117	295.44	-0.052	0.075	51.3	50.7	303.7	242.0
	IT18 17/2/67118	303.14	-0.093	0.039	51.6	51.0	322.4	256.9
	IT18 17/2/67119	295.69	-0.073	0.055	51.6	51.0	304.5	242.6
	IT18 20/2/67123	296.81	-0.029	0.100	51.9	51.1	303.9	242.1
	IT18 20/2/67124	298.29	-0.005	0.125	51.8	51.0	309.5	246.6
	IT18 20/2/67125	294.61	-0.076	0.055	51.6	51.0	309.5	246.6
	IT18 20/2/67126	294.40	-0.155	0.009	51.6	51.0	390.1	310.9

(*) Experiments with Run No ≥ 103 have been carried out after polishing of the test section (see 6.1.).

CRITICAL POWER – IETI3 ... PLANT – ELIT.22-a TABLE 5....

REMARKS – RUN. No.	G	X_{in}	X_o	P_{in}	P_o	W	ϕ
	g/cm² s	by weight		kg/cm² abs		kW	W/cm²
ox IT22 1/6/67 66	38.78	-0.195	0.825	51.7	51.4	318.7	169.2
IT22 1/6/67 67	41.59	-0.062	0.826	51.2	50.9	298.8	158.7
IT22 1/6/67 68	43.09	-0.004	0.767	51.5	51.2	268.7	142.7
IT22 24/5/67 28	77.57	-0.172	0.523	51.6	51.3	435.4	231.2
IT22 24/5/67 29	77.40	-0.124	0.534	52.2	51.9	410.2	217.8
IT22 24/5/67 26	79.75	-0.069	0.559	51.3	51.0	405.5	215.3
IT22 24/5/67 27	79.93	-0.080	0.556	51.3	51.0	411.2	218.3
IT22 24/5/67 30	80.64	-0.025	0.549	51.1	50.8	374.8	199.0
IT22 24/5/67 31	79.46	-0.022	0.553	50.3	50.0	371.1	197.1
IT22 30/5/67 36	111.74	-0.207	0.347	32.0	31.3	544.8	289.3
IT22 29/5/67 35	110.84	-0.170	0.376	31.4	30.8	534.9	284.0
IT22 29 5/67 33	110.09	-0.121	0.409	31.5	31.0	516.5	274.3
ox IT22 29 5/67 34	110.01	-0.120	0.392	31.3	30.8	498.5	264.7
IT22 30 5/67 37	109.29	-0.047	0.436	31.4	30.8	466.4	247.7
IT22 30 5/67 38	110.22	-0.021	0.446	31.6	31.0	455.3	241.8
IT22 23 5/67 22	106.19	-0.278	0.315	51.2	50.9	509.1	270.3
IT22 23 5/67 23	108.01	-0.198	0.353	51.3	51.0	480.8	255.3
IT22 23 5/67 1	112.52	-0.143	0.370	51.1	50.8	467.4	248.2
IT22 23 5/67 2	107.11	-0.151	0.390	51.3	51.0	468.5	248.7
IT22 23 5/67 24	106.83	-0.129	0.395	51.3	51.0	452.3	240.2
IT22 1/6/67 65	106.82	-0.073	0.420	51.3	51.0	425.6	226.0
IT22 23 5/67 25	111.65	-0.041	0.419	51.3	51.0	415.0	220.4
IT22 30 5/67 39	111.24	-0.216	0.311	61.1	60.7	454.3	241.2
IT22 30 5/67 40	117.99	-0.170	0.305	62.5	62.1	432.5	229.6
IT22 30 5/67 41	115.47	-0.101	0.351	61.2	60.8	404.5	214.8
IT22 30 5/67 42	112.42	-0.033	0.393	61.5	61.1	370.2	196.6
IT22 30/5/67 43	224.42	-0.146	0.154	31.6	30.9	593.1	314.9
IT22 30/5/67 44	223.59	-0.097	0.195	31.9	31.1	571.5	303.4
IT22 30/5/67 45	225.50	-0.097	0.190	32.2	31.5	567.0	301.1
IT22 30/5/67 46	221.69	-0.039	0.231	32.2	31.2	521.9	277.1
IT22 23/5/67 20	216.86	-0.257	0.073	50.3	50.0	579.4	307.6
IT22 18/5/67 4	221.73	-0.212	0.100	51.4	51.0	558.0	296.3
IT22 18/5/67 5	219.97	-0.187	0.115	51.4	51.0	537.1	285.2
IT22 1/6/67 64	220.00	-0.139	0.146	51.7	51.2	504.8	268.1
IT22 24/5/67 32	218.29	-0.140	0.150	51.4	51.0	512.3	272.0
IT22 18/5/67 6	212.31	-0.090	0.193	50.4	50.0	486.0	258.0
IT22 18/5/67 3	224.91	-0.137	0.140	52.0	51.5	500.6	265.8
IT22 23/5/67 21	224.74	-0.032	0.210	50.8	50.5	439.3	233.3
IT22 1/6/67 63	217.44	-0.236	0.071	61.4	61.0	515.5	273.7
IT22 30/5/67 47	225.12	-0.189	0.085	61.9	61.4	475.6	252.5
IT22 1/6/67 59	221.21	-0.135	0.129	62.0	61.5	450.3	239.1
IT22 1/6/67 60	229.38	-0.086	0.154	61.7	61.2	424.7	225.5
IT22 1/6/67 62	227.31	-0.045	0.190	61.5	61.0	413.1	219.3
IT22 1/6/67 61	223.81	-0.029	0.200	62.4	61.9	396.1	210.3
IT22 22/5/67 12	293.33	-0.191	0.034	51.4	51.0	533.8	283.4
IT22 22/5/67 11	292.09	-0.158	0.060	52.2	51.8	512.3	272.0
IT22 22/5/67 10	301.23	-0.094	0.098	51.5	51.0	466.4	247.7
IT22 19/5/67 8	300.59	-0.090	0.104	52.2	51.3	466.4	247.7
IT22 22/5/67 13	301.05	-0.029	0.155	51.7	51.0	445.3	236.4
IT22 23/5/67 14	296.82	-0.233	0.011	51.4	51.0	582.8	309.4

CRITICAL POWER - IETI 3...PLANT - ELIT 22-a TABLE 5 (cont)

REMARKS - RUN. No.	G	X_{in}	X_e	P_{in}	P_e	W	ϕ
	g/cm² s	by weight		kg/cm² abs		kW	W/cm²
IT22 23/5/67 18	374.86	-0.195	0.004	51.5	51.0	599.9	318.6
IT22 23/5/67 17	377.39	-0.148	0.028	51.5	51.0	534.9	284.0
IT22 23/5/67 19	383.98	-0.113	0.044	50.4	50.0	489.1	259.7
IT22 23/5/67 15	377.13	-0.081	0.069	52.2	51.5	452.3	240.2
IT22 23/5/67 16	379.12	-0.026	0.125	51.2	50.2	454.3	241.2

CRITICAL POWER - IETI 3...PLANT - ELIT 22-f TABLE 6....

REMARKS - RUN. No.	G	X_{in}	X_e	P_{in}	P_e	W	ϕ
	g/cm² s	by weight		kg/cm² abs		kW	W/cm²
IT22 31/5/67 53	219.38	-0.192	0.042	51.5	51.2	413.5	329.5
IT22 31/5/67 54	213.59	-0.128	0.092	51.4	51.0	377.9	301.1
IT22 31/5/67 55	221.50	-0.090	0.109	51.3	50.9	356.6	284.1
IT22 31/5/67 56	229.17	-0.063	0.126	51.4	51.0	347.9	277.2
IT22 31/5/67 57	227.69	-0.024	0.159	51.8	51.4	335.4	267.3
IT22 31/5/67 52	290.53	-0.201	-0.015	51.2	50.7	430.9	343.3
IT22 31/5/67 58	313.02	-0.152	0.002	51.5	51.0	385.1	306.8
IT22 31/5/67 48	292.09	-0.145	0.022	51.5	51.0	391.9	312.2
IT22 31/5/67 49	292.46	-0.101	0.050	51.5	51.0	354.8	282.7
IT22 31/5/67 50	295.91	-0.049	0.094	51.5	51.0	339.7	270.7
IT22 31/5/67 51	302.38	-0.015	0.123	52.2	51.6	332.3	264.8

Appendix TABLE 7 (extracted from table $^{1}/_{1}$ of ref (3))

CRITICAL HEAT FLUX - IETI 2 - PLANT-EL G1-a

RUN No	G	P_o	ΔP	X_{in}	X_o	W	ϕ
	$g/cm^2\ s$	kg/cm^2 abs	kg/cm^2	by weight		kW	W/cm^2
420	108	51.2	0.32	-0.081	0.377	399.4	213.2
421	108	51.2	0.32	-0.085	0.381	403.2	215.2
422	111	51.3	0.32	-0.139	0.344	430.0	229.5
423	111	51.1	0.32	-0.139	0.348	430.6	229.8
449	110	51.0	0.31	-0.206	0.307	452.1	241.3
450	110	51.0	0.31	-0.206	0.305	450.7	240.5
424	219	51.4	0.50	-0.090	0.159	432.1	236.0
425	221	50.9	0.50	-0.090	0.157	436.0	232.7
434	217	51.1	0.45	-0.144	0.123	459.2	245.1
435	218	51.1	0.45	-0.145	0.122	460.7	245.9
436	215	51.1	0.39	-0.204	0.083	487.8	260.3
437	218	50.9	0.39	-0.206	0.076	488.9	269.0
426	300	51.9	0.53	-0.098	0.089	432.0	230.6
427	303	51.5	0.53	-0.102	0.082	436.3	232.8
432	300	51.1	0.48	-0.128	0.061	457.7	244.3
433	301	51.2	0.48	-0.109	0.058	456.1	243.4
438	293	51.4	0.42	-0.195	0.023	505.2	269.6
439	293	51.4	0.42	-0.196	0.023	508.2	271.2
428	375	51.4	0.59	-0.095	0.053	431.7	230.4
429	376	51.5	0.59	-0.096	0.063	431.7	230.4
430	376	50.9	0.51	-0.143	0.023	496.6	265.0
431	380	50.9	0.52	-0.143	0.022	498.4	266.0
451	379	51.4	0.45	-0.203	-0.004	594.3	317.2
452	379	51.4	0.45	-0.203	-0.005	592.9	316.4

TABLE 8 (extracted from table 1/6 of ref. (3))

CRITICAL HEAT FLUX - IETI 2 - PLANT - EL G1-F

RUN No	G	P_0	ΔP	X_{in}	X_0	W	ϕ
	$g/cm^2 s$	kg/cm^2 abs	kg/cm^2	by weight		kW	W/cm^2
455	221	50.9	0.30	-0.095	0.090	328.7	263.2
456	220	50.9	0.30	-0.095	0.090	326.1	261.1
463	218	50.9	0.26	-0.159	0.045	358.2	286.8
464	221	50.9	0.26	-0.168	0.035	358.9	287.3
469	214	50.9	0.25	-0.188	0.032	375.4	300.6
470	215	50.9	0.25	-0.189	0.036	384.2	307.6
457	292	50.9	0.33	-0.096	0.045	328.7	263.2
458	296	50.9	0.33	-0.095	0.043	326.1	261.1
465	300	51.2	0.30	-0.148	0.012	379.2	303.6
466	300	51.3	0.30	-0.147	0.012	375.8	300.8
471	301	51.2	0.29	-0.210	-0.035	424.0	339.4

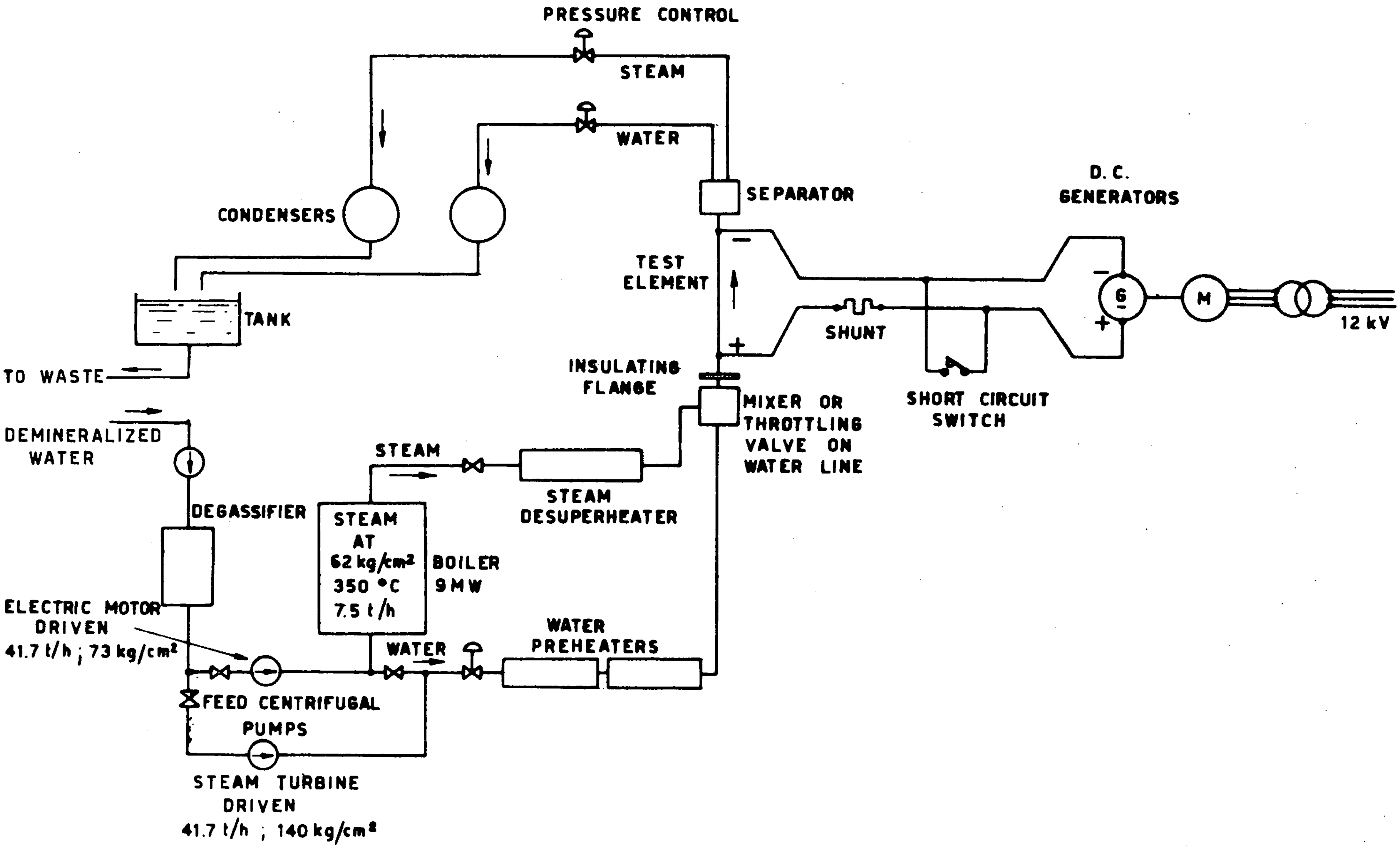

Fig. 1 - Schematic diagram of CISE IETI-2 plant (Genoa).

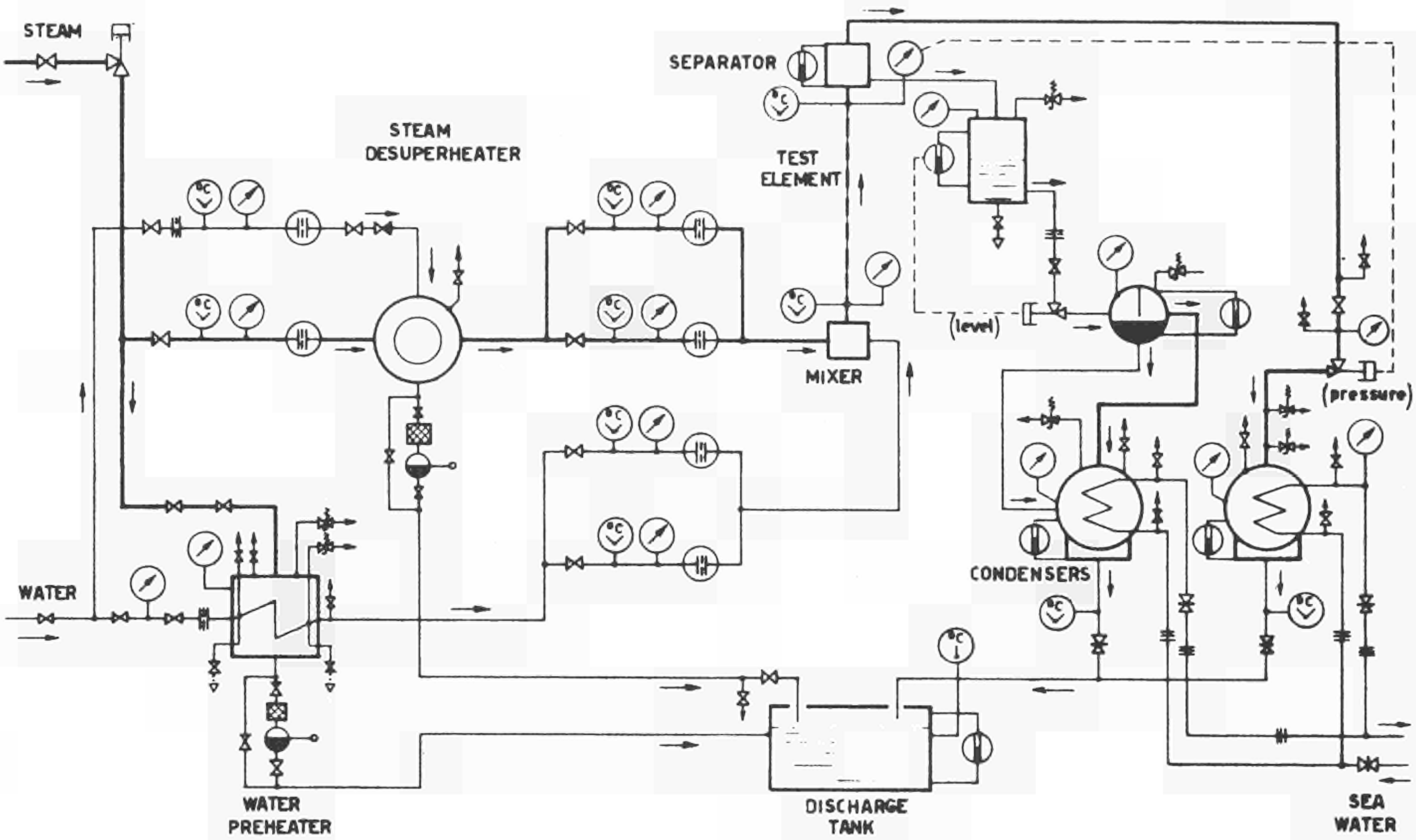

Fig. 2 — Hydraulic section of CISE IETI-2 plant.

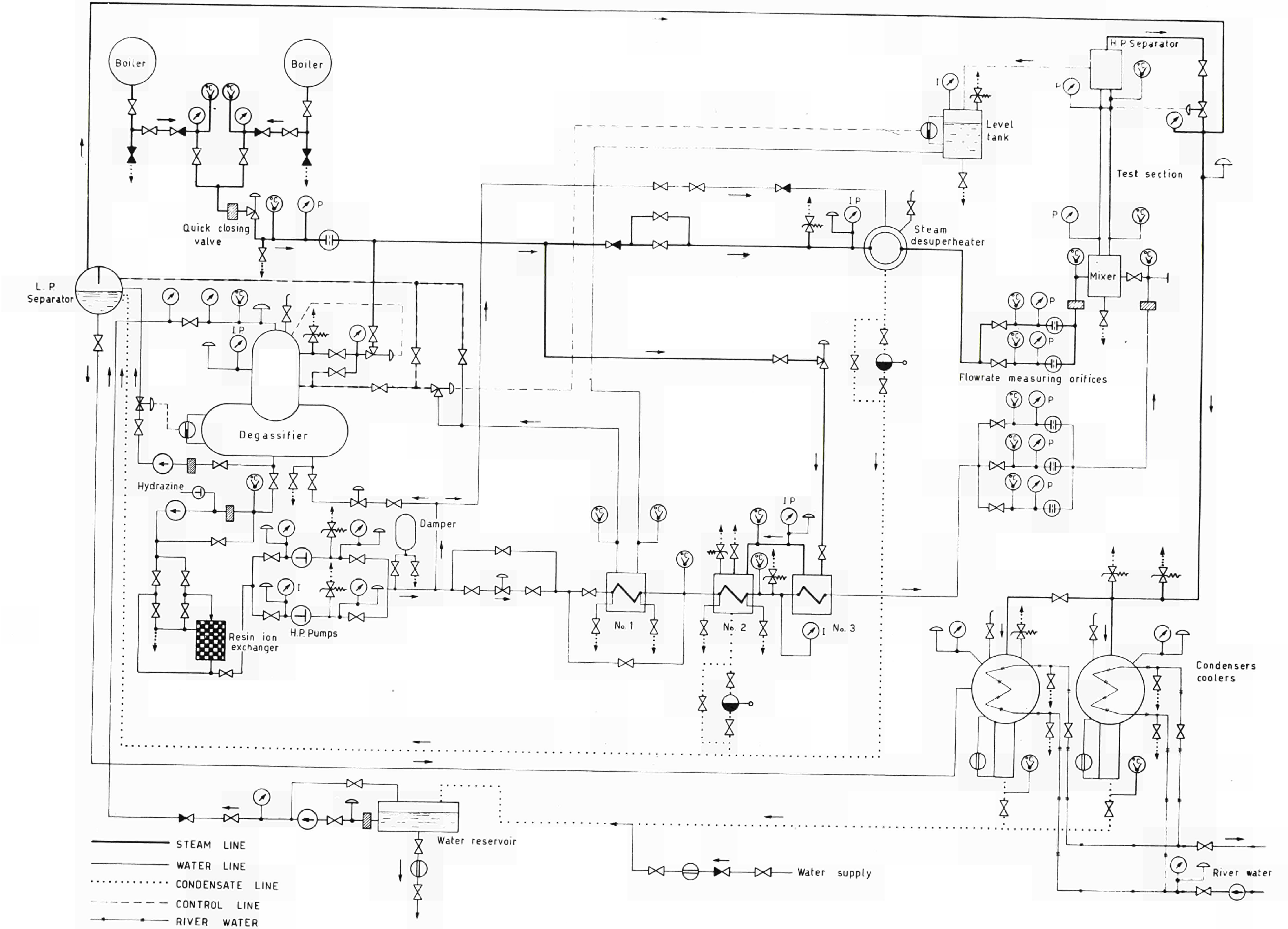

Fig. 3 – CISE IETI-3 Plant Piacenza – Hydraulic section .

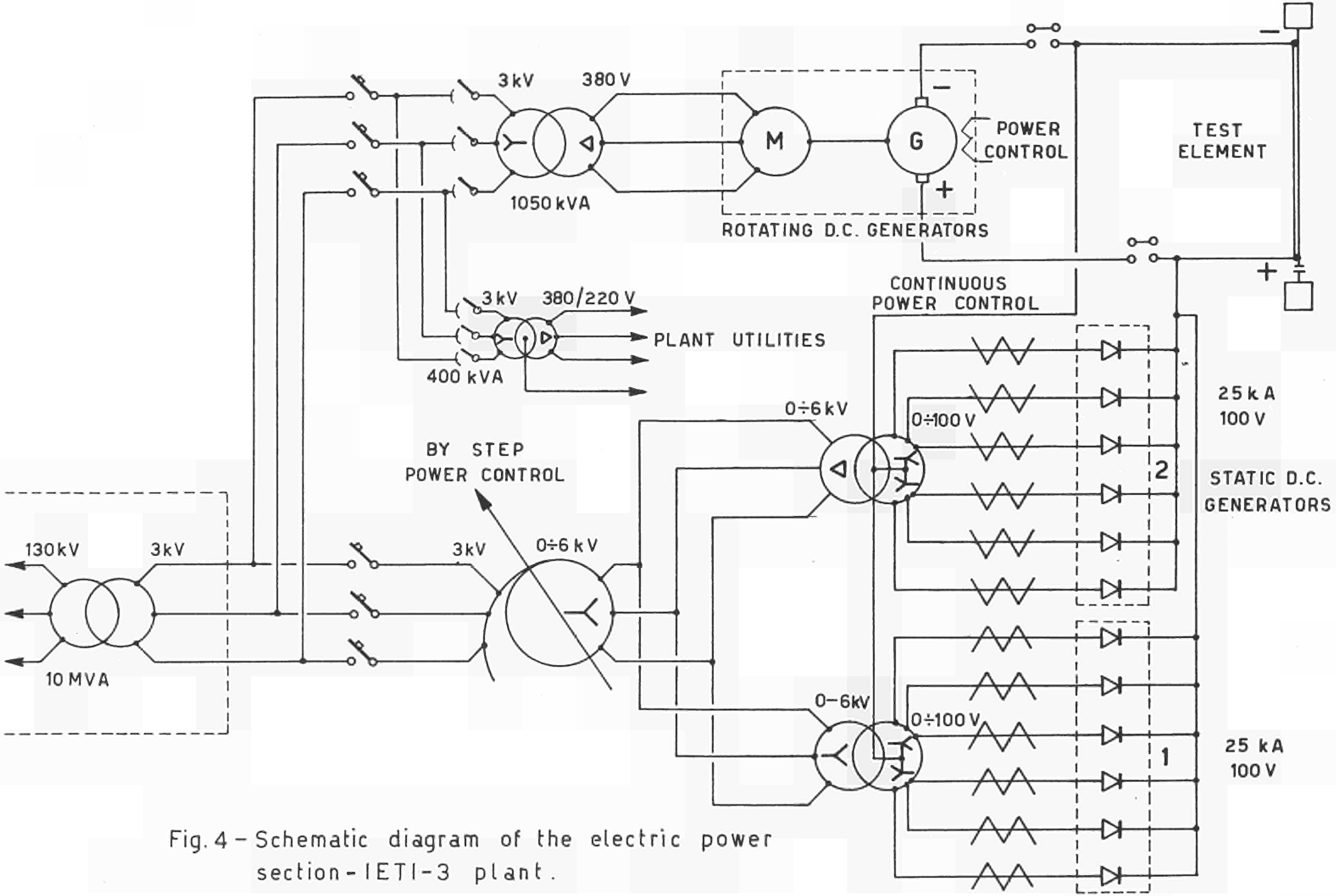

Fig. 4 - Schematic diagram of the electric power section - IETI-3 plant.

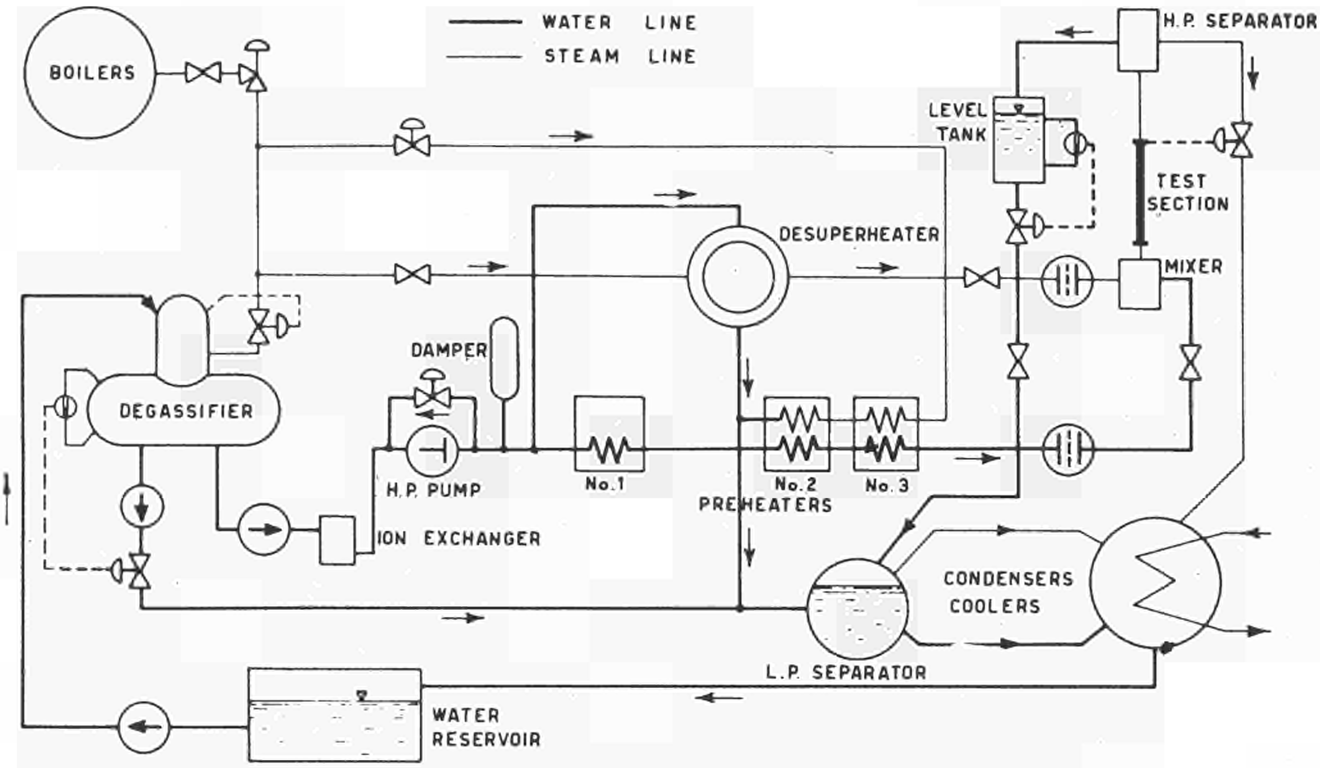

Fig. 5 a) - Scheme of the IETI 3 circuit for flowrate $\lesssim$ 20 t/h (open-loop scheme).

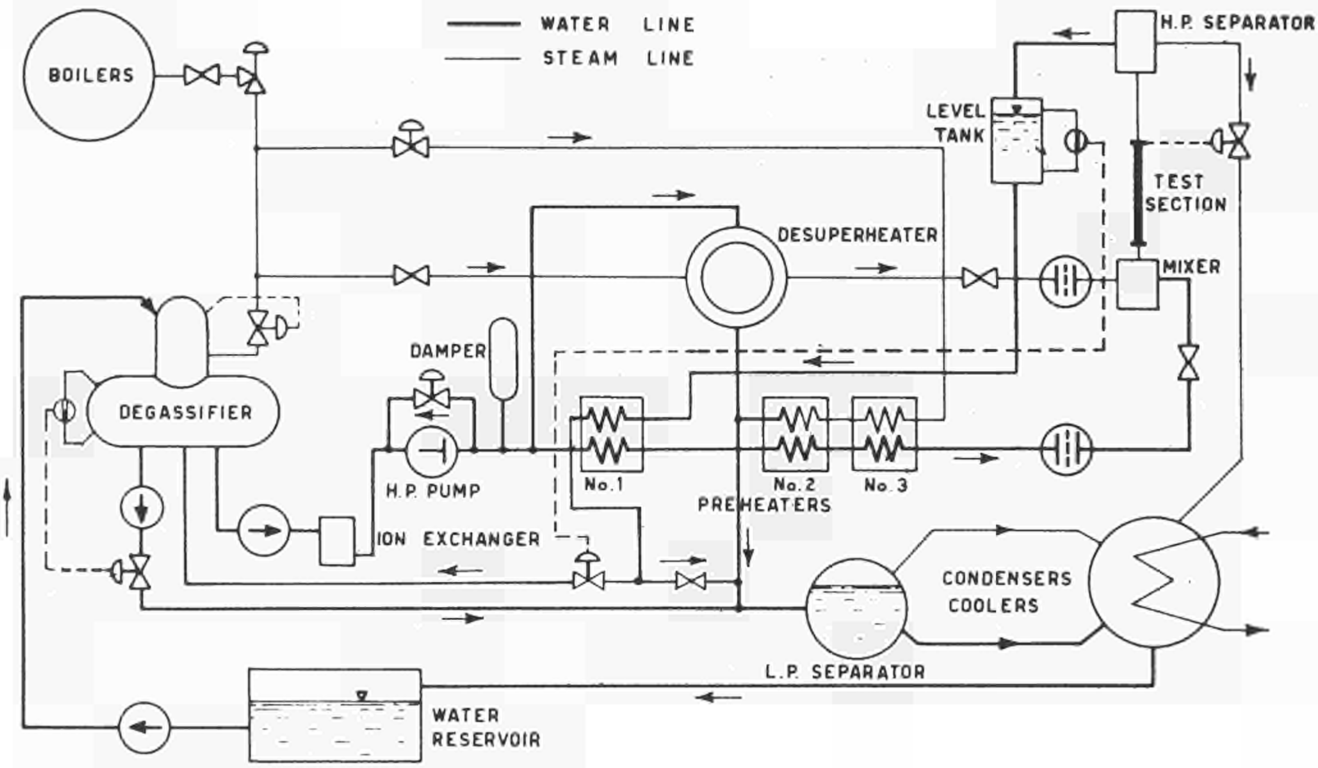

Fig. 5 b) - Scheme of the IETI 3 circuit for flowrate $\gtrsim$ 20 t/h (semi-open loop scheme).

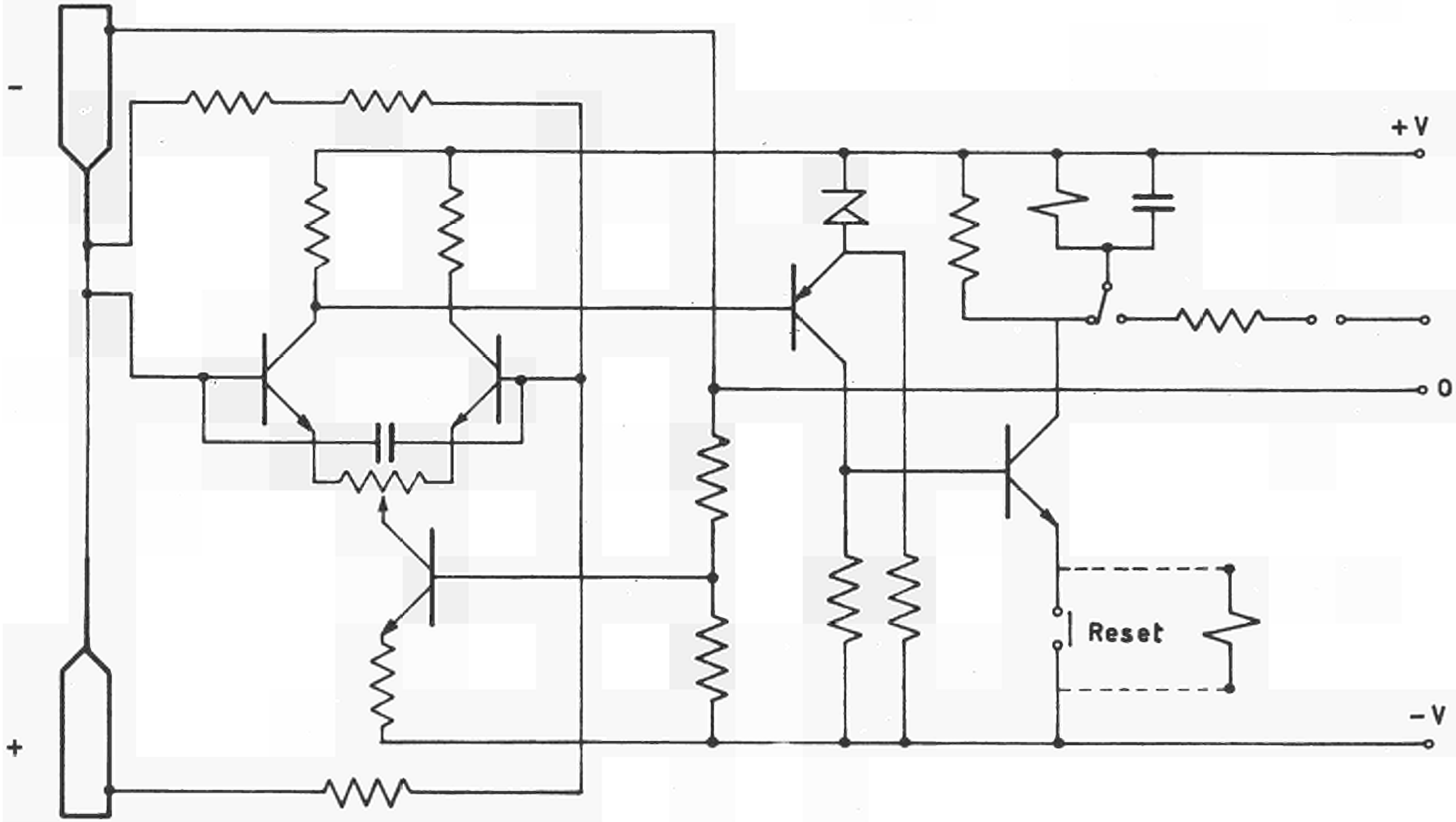

Fig. 6–Circuit of the burn-out detector.

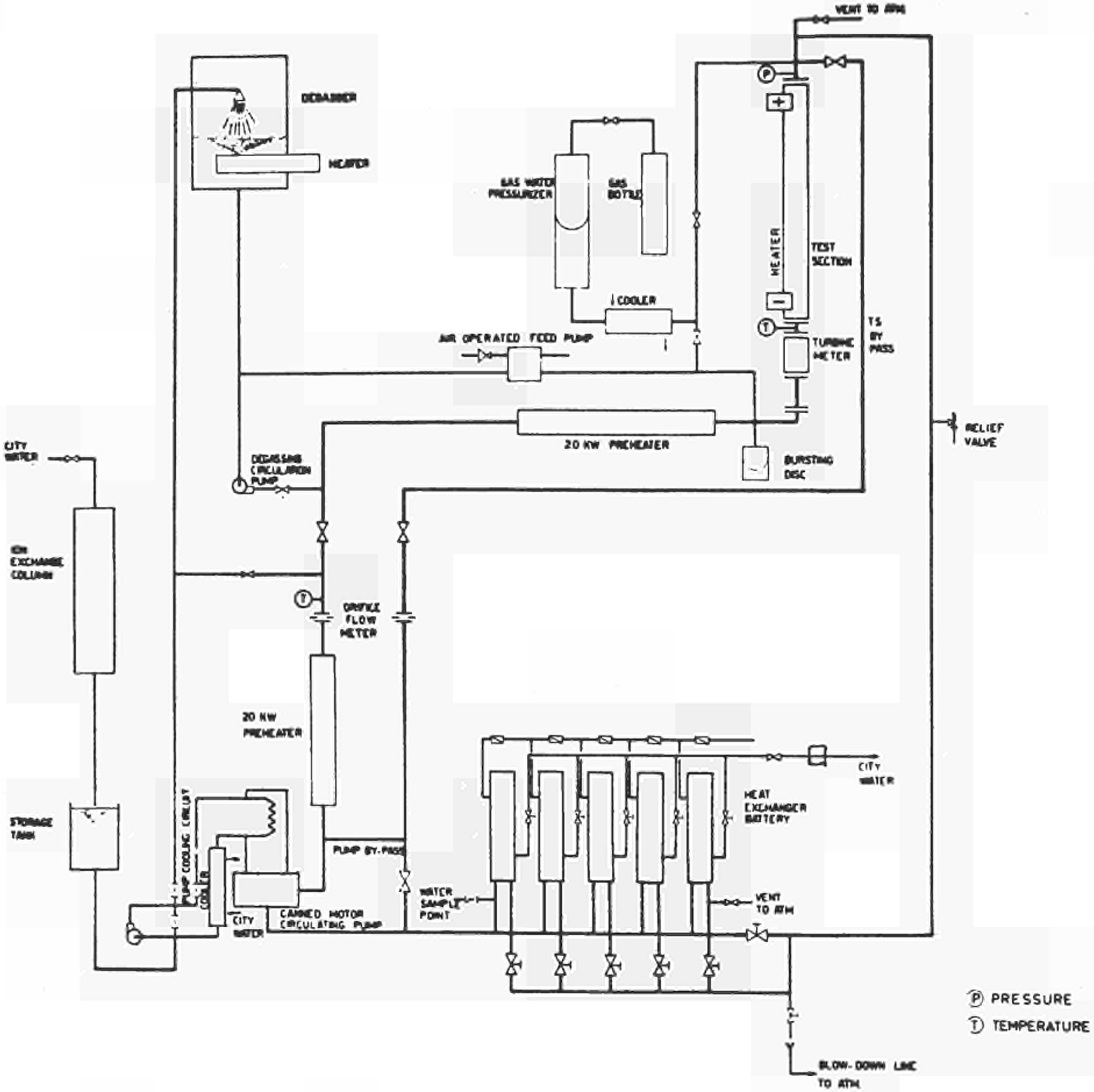

Fig.7-SORIN High Pressure Facility (Saluggia).

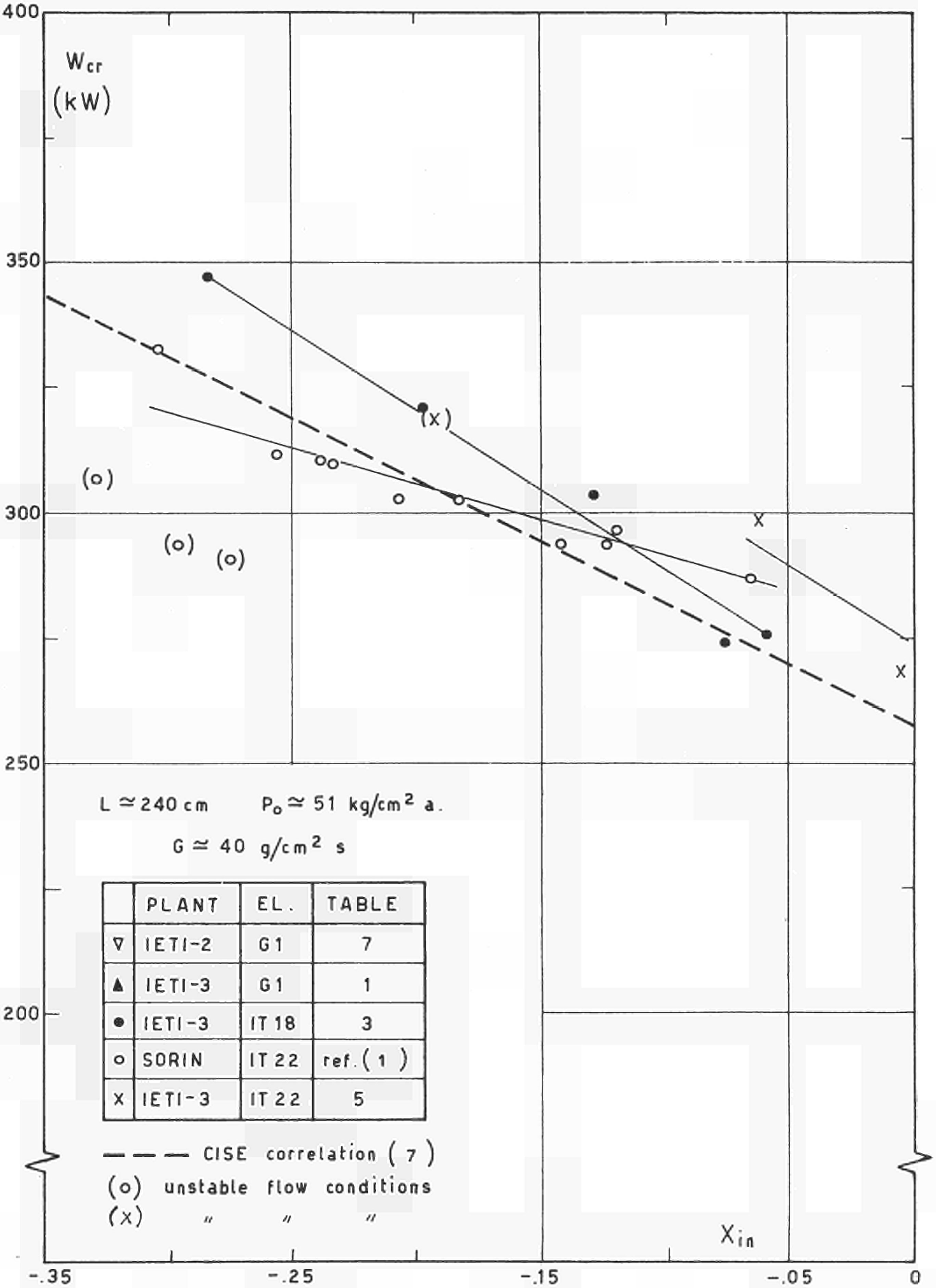

Fig. 8 – Critical Power vs. inlet quality.

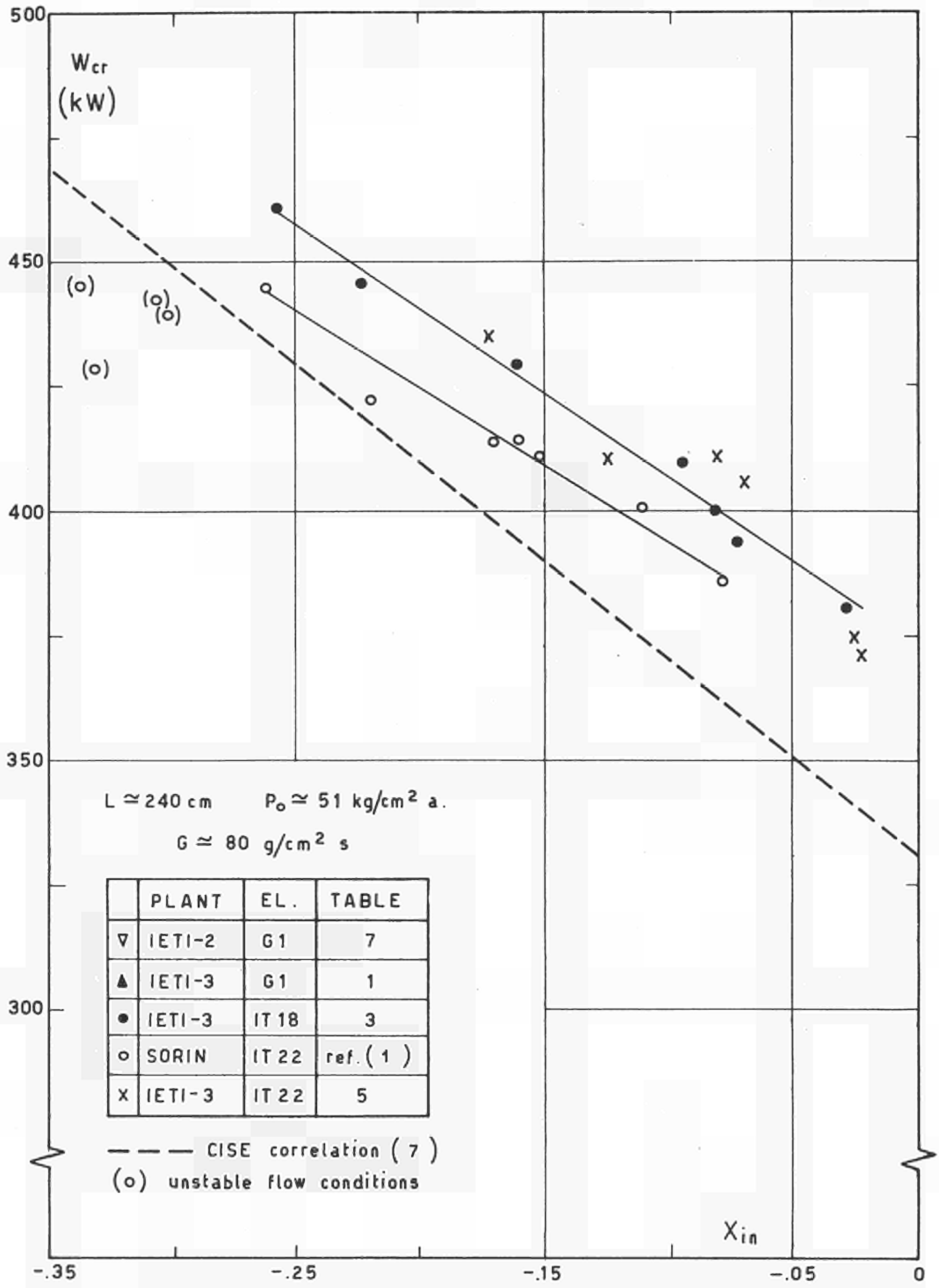

Fig.9 – Critical Power vs. inlet quality.

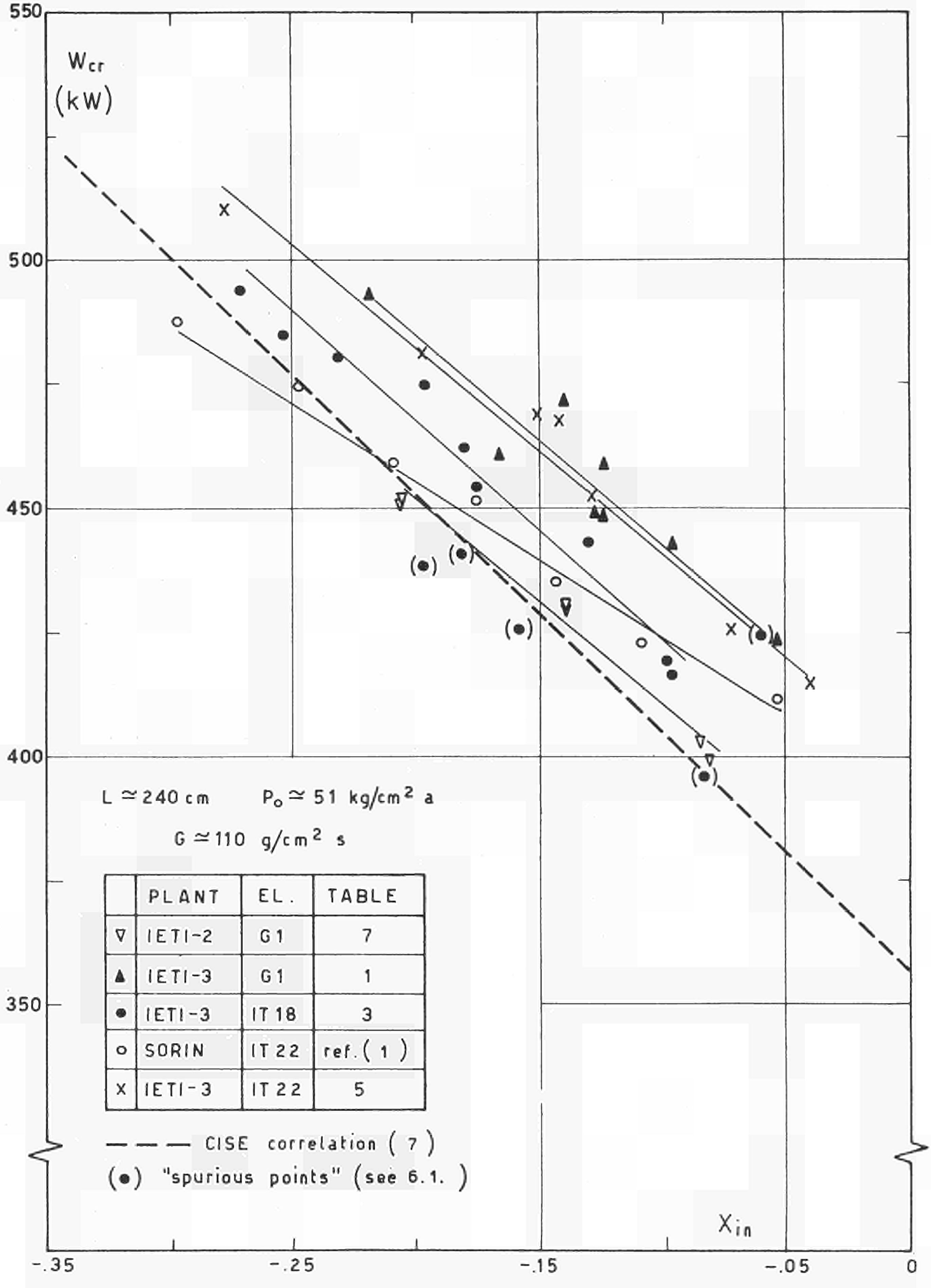

Fig.10 – Critical Power vs. inlet quality.

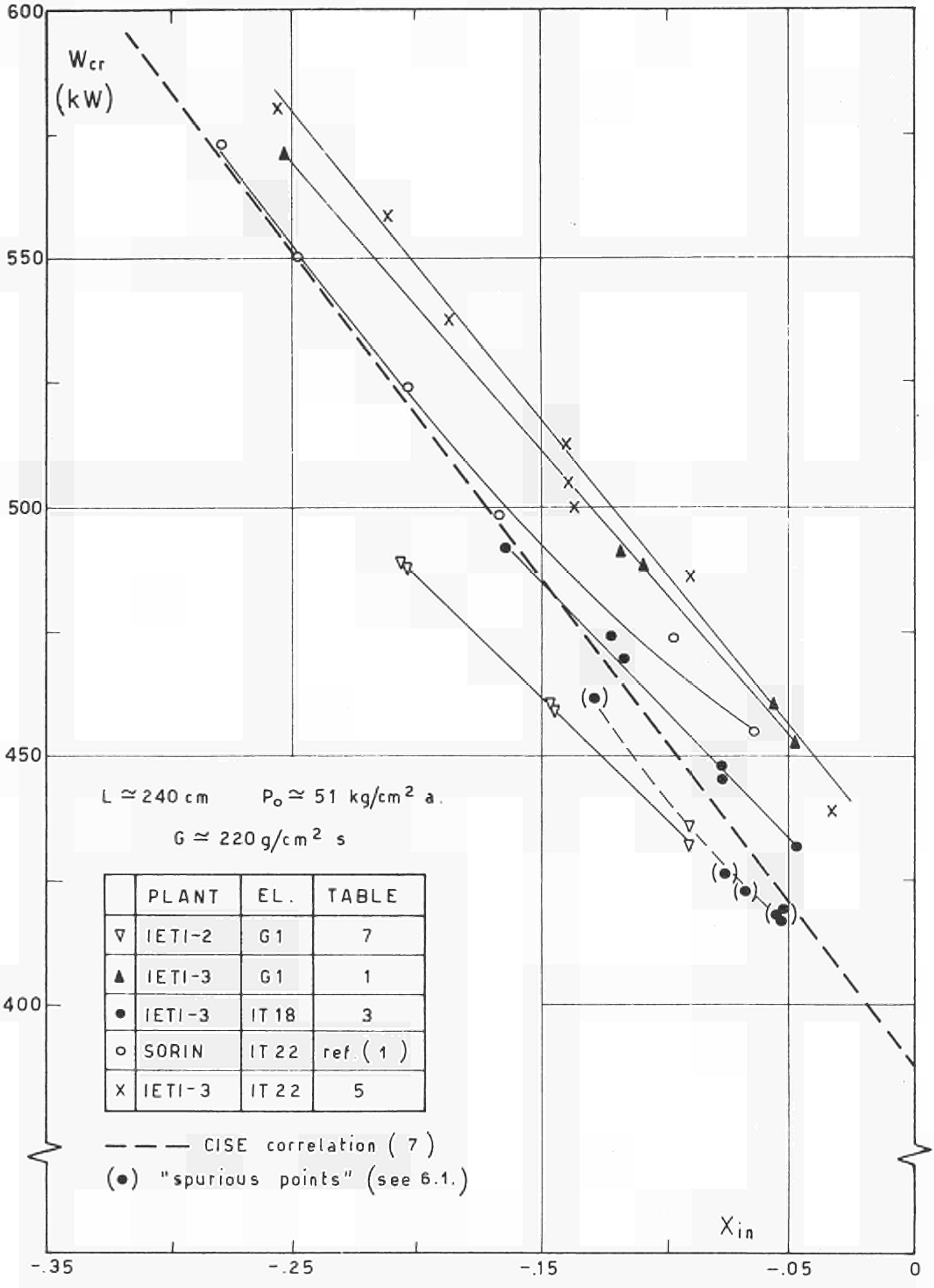

Fig. 11 – Critical Power vs. inlet quality.

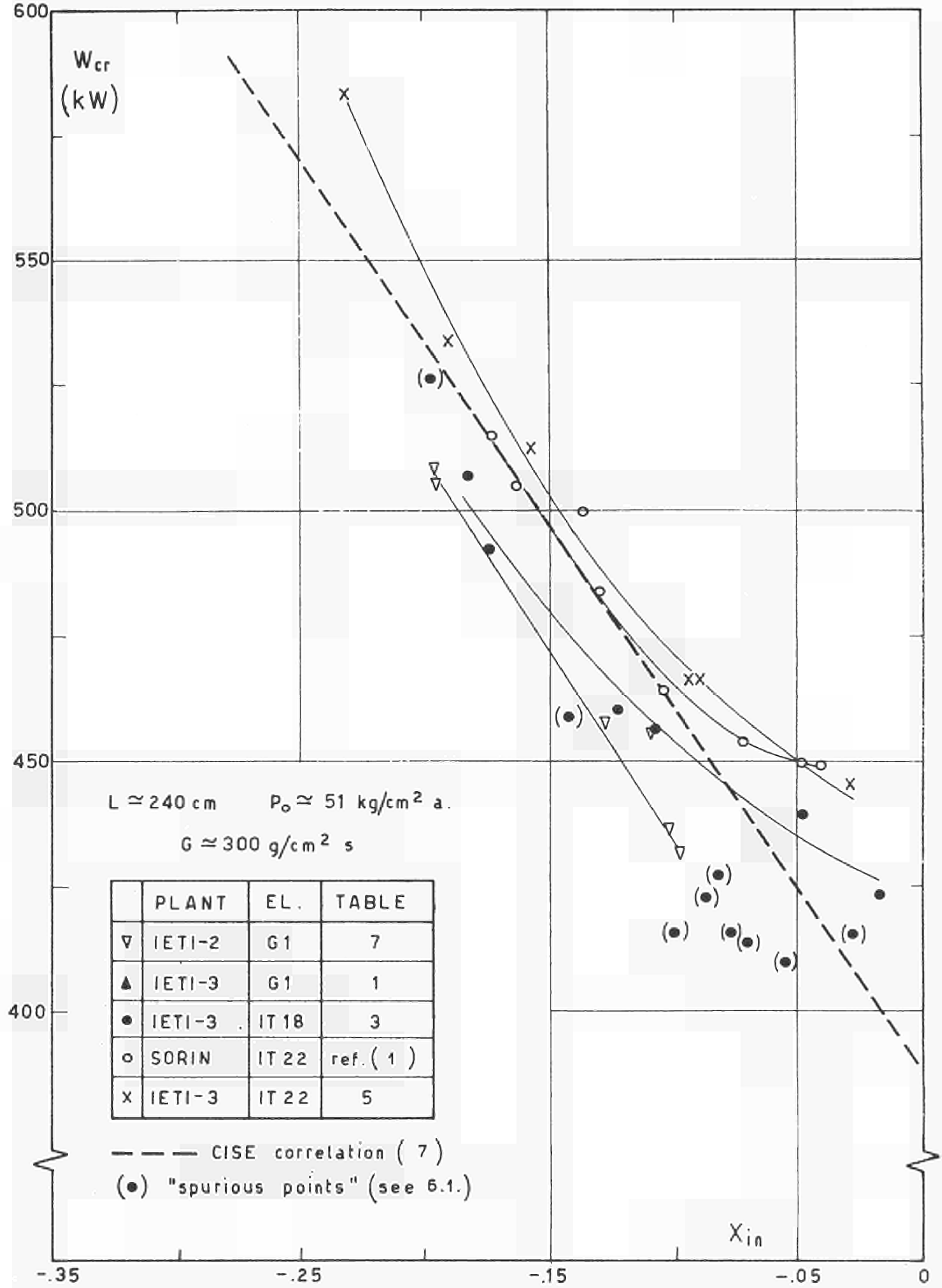

Fig. 12 – Critical Power vs. inlet quality.

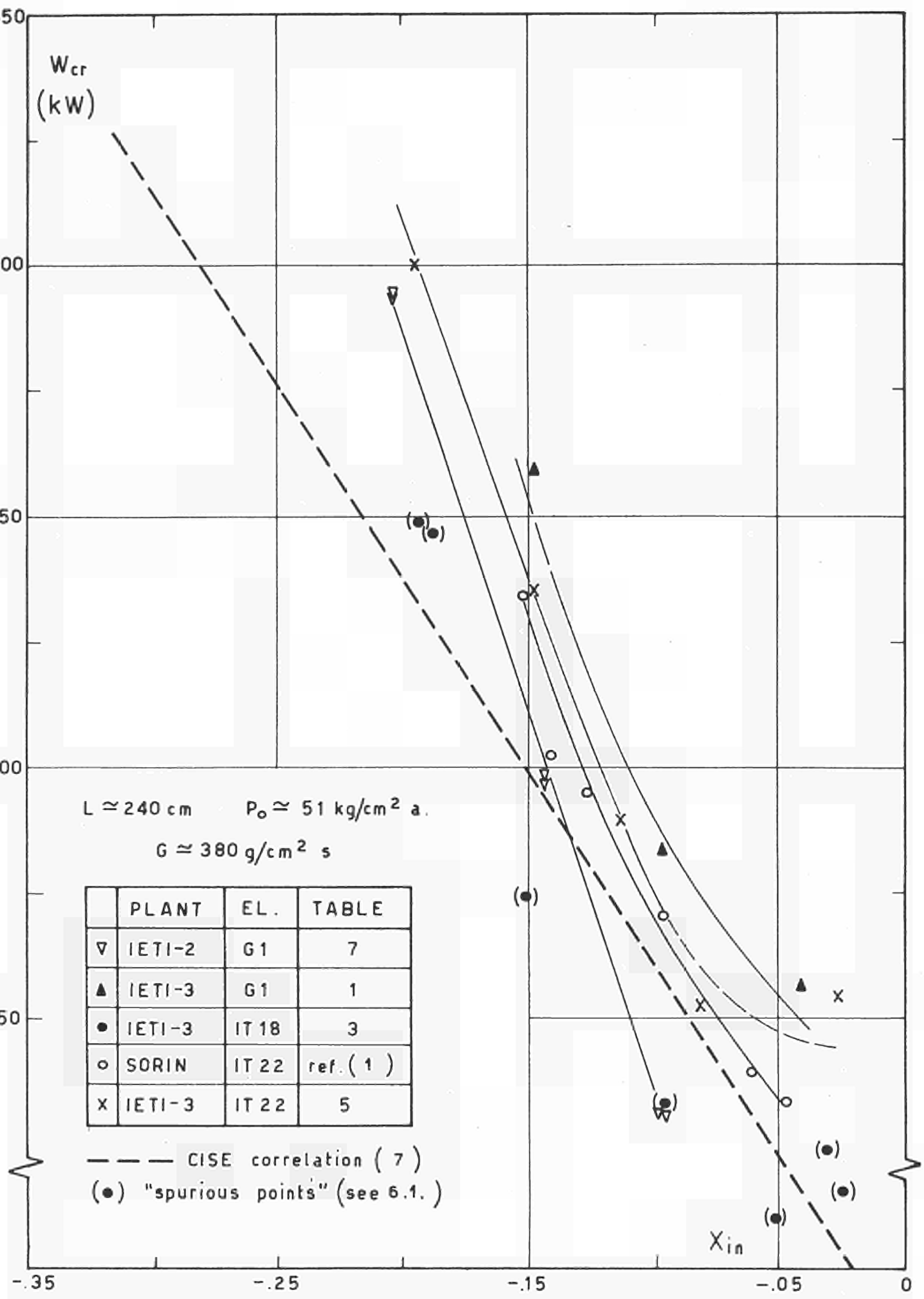

Fig.13 — Critical Power vs. inlet quality.

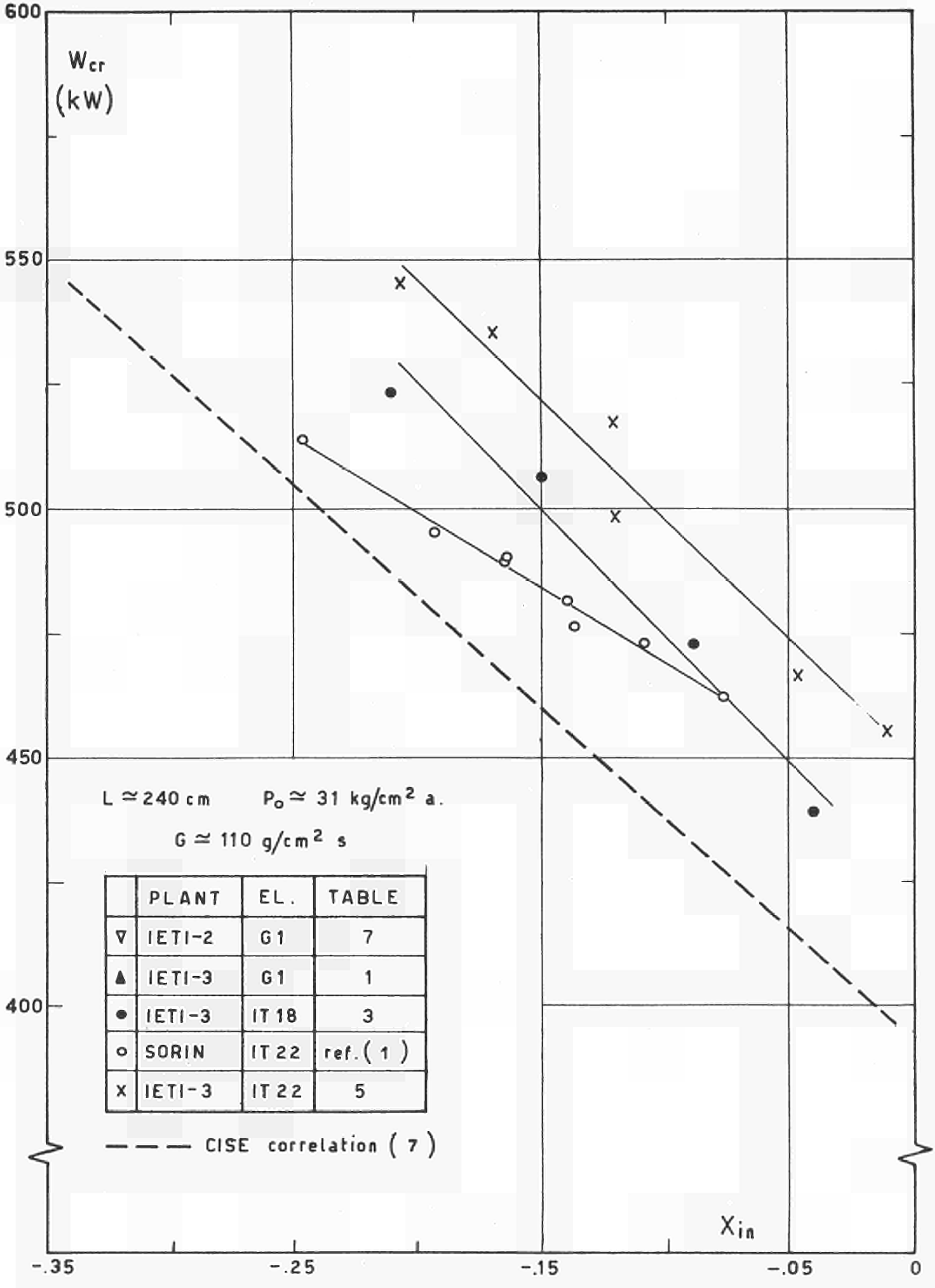

Fig. 14 – Critical Power vs. inlet quality.

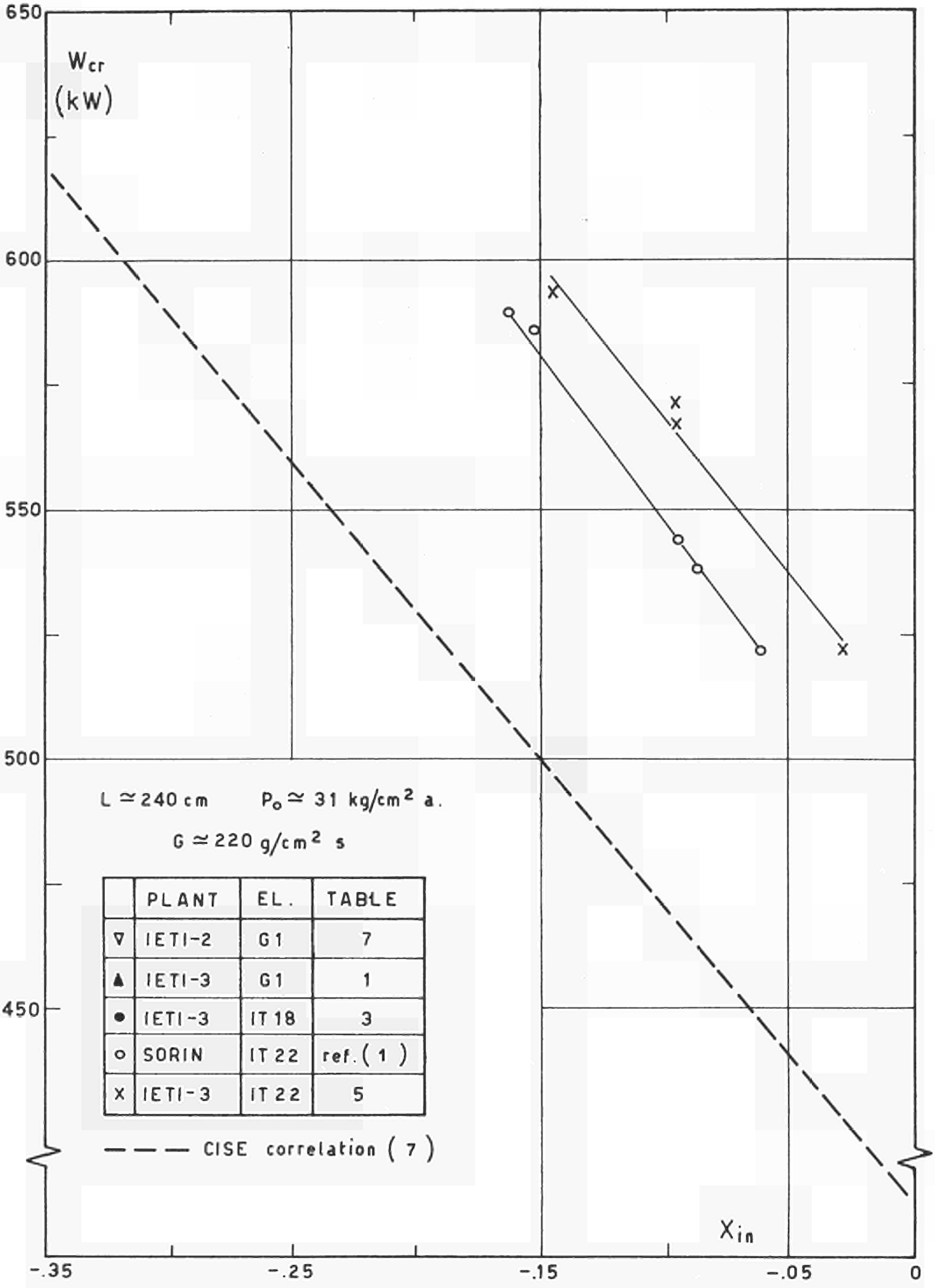

Fig. 15 – Critical Power vs. inlet quality.

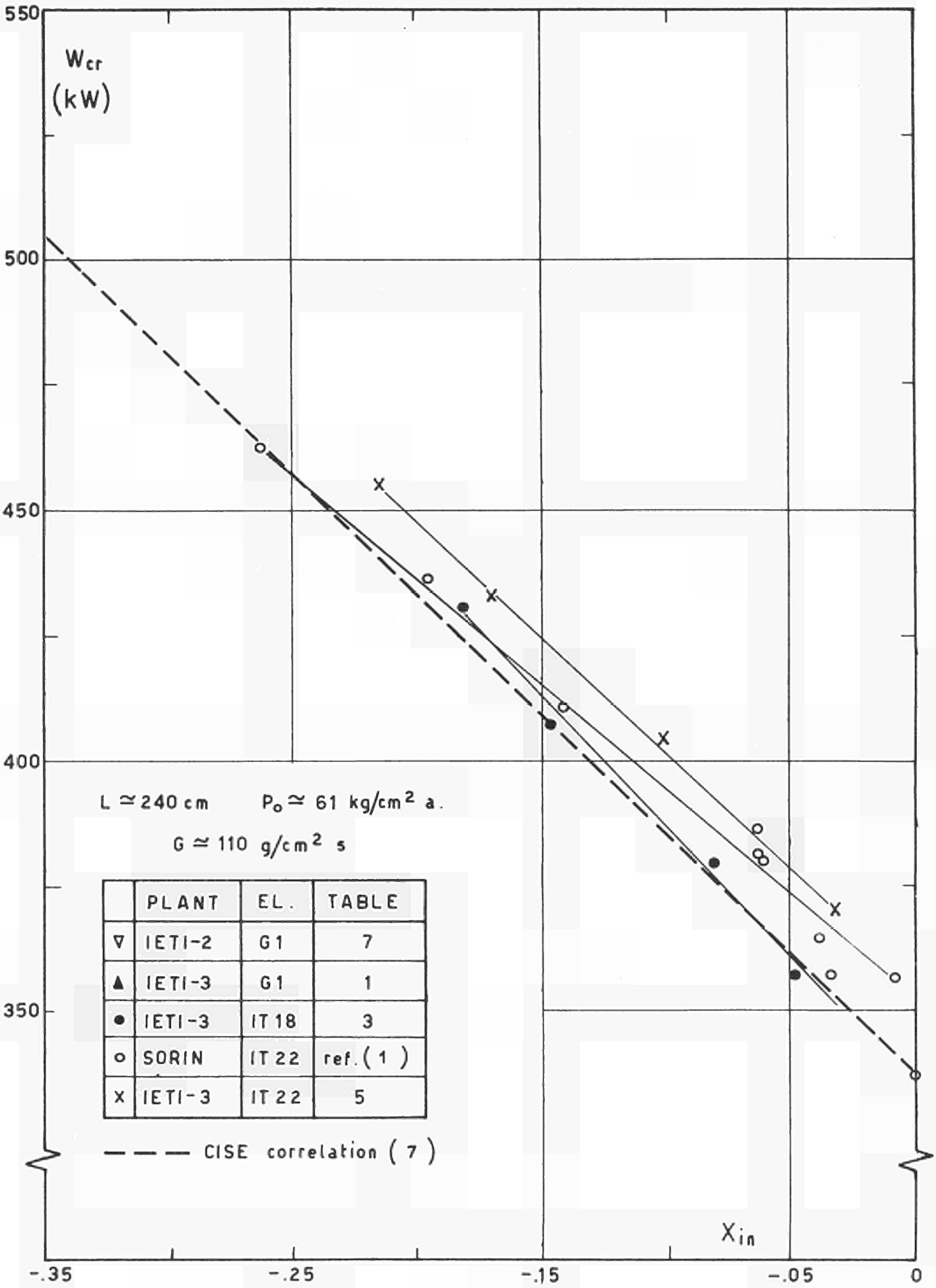

Fig.16 — Critical Power vs. inlet quality.

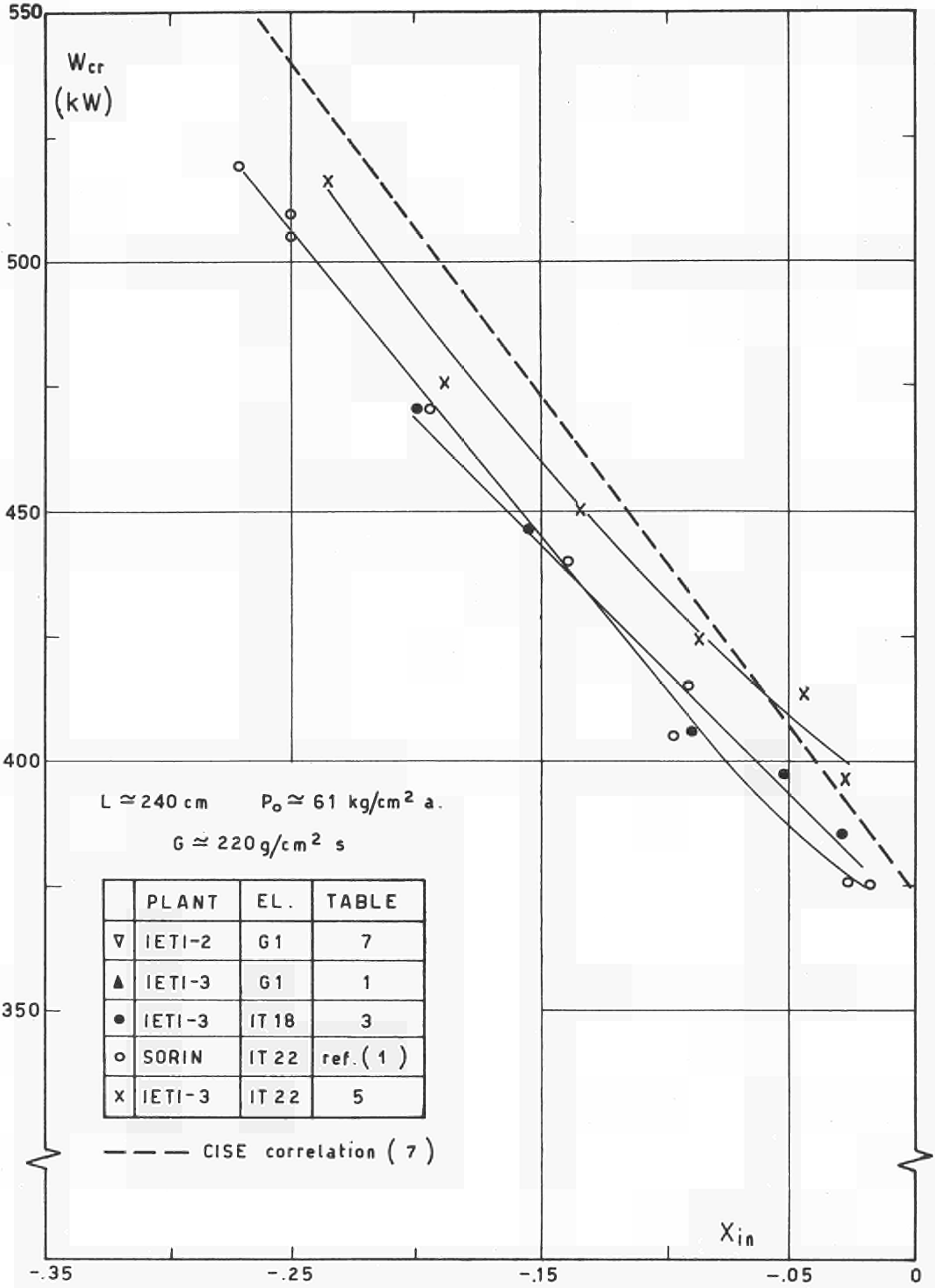

Fig. 17 – Critical Power vs. inlet quality.

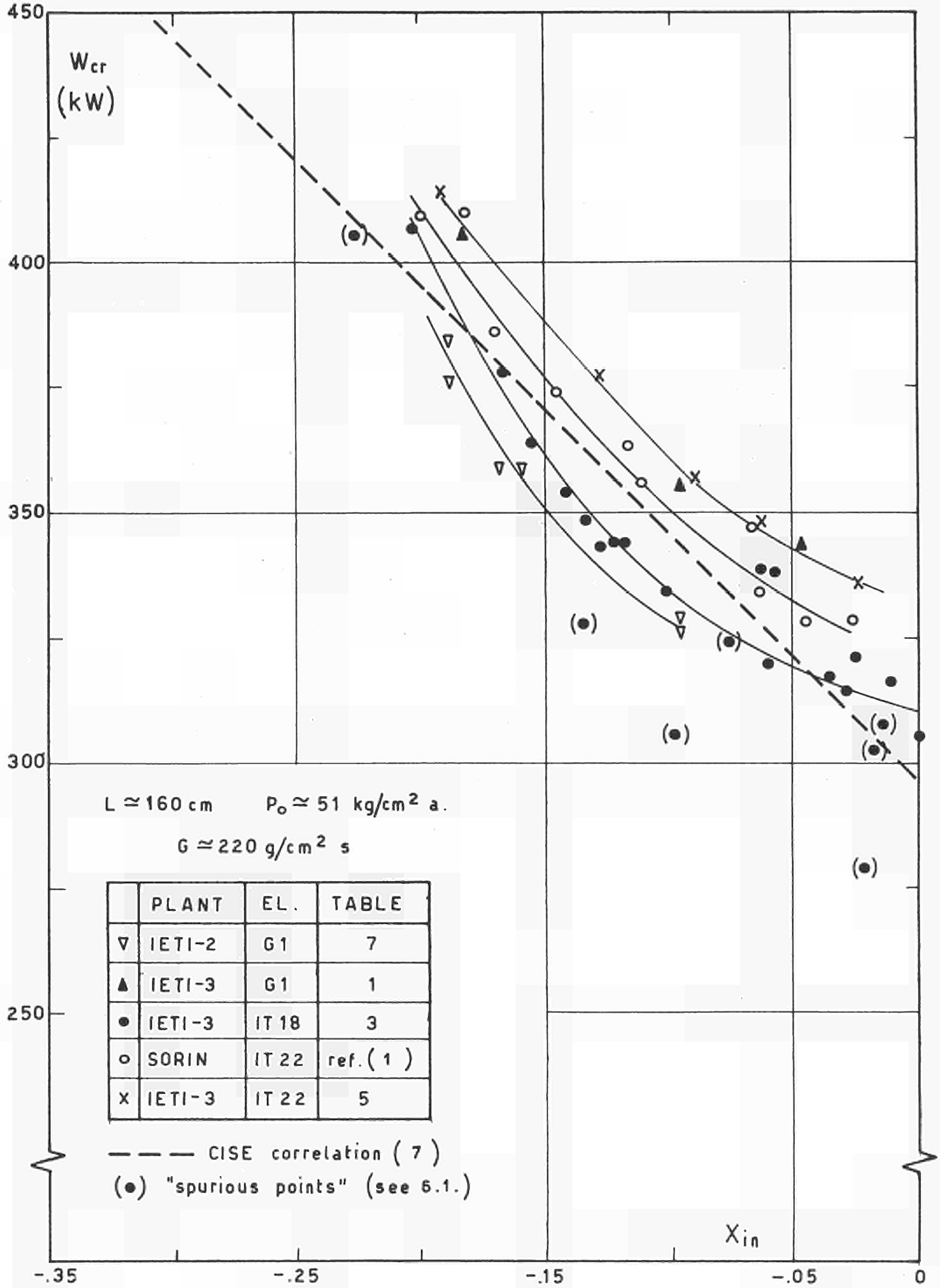

Fig. 18 – Critical Power vs. inlet quality.

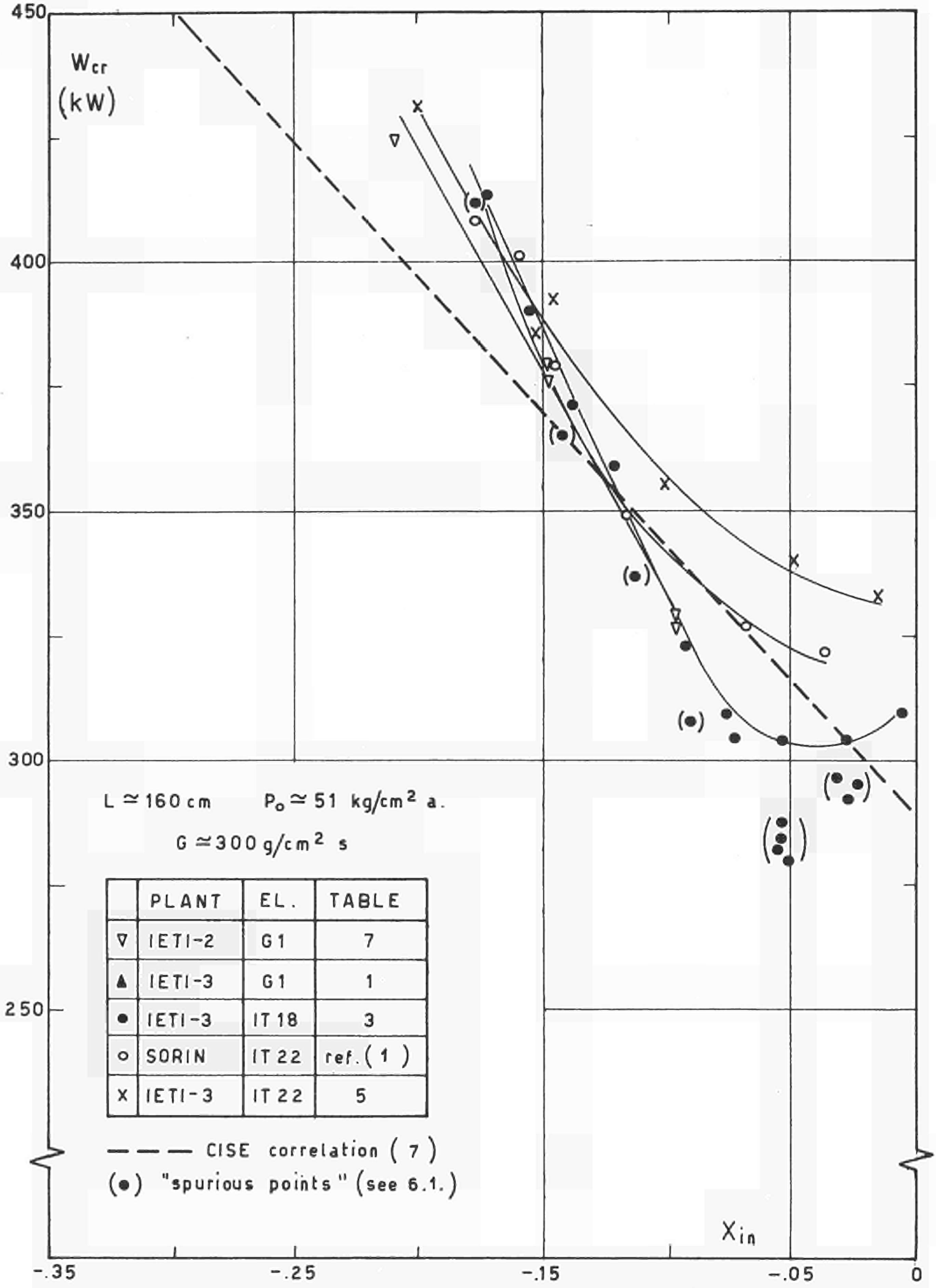

Fig.19 – Critical Power vs. inlet quality.

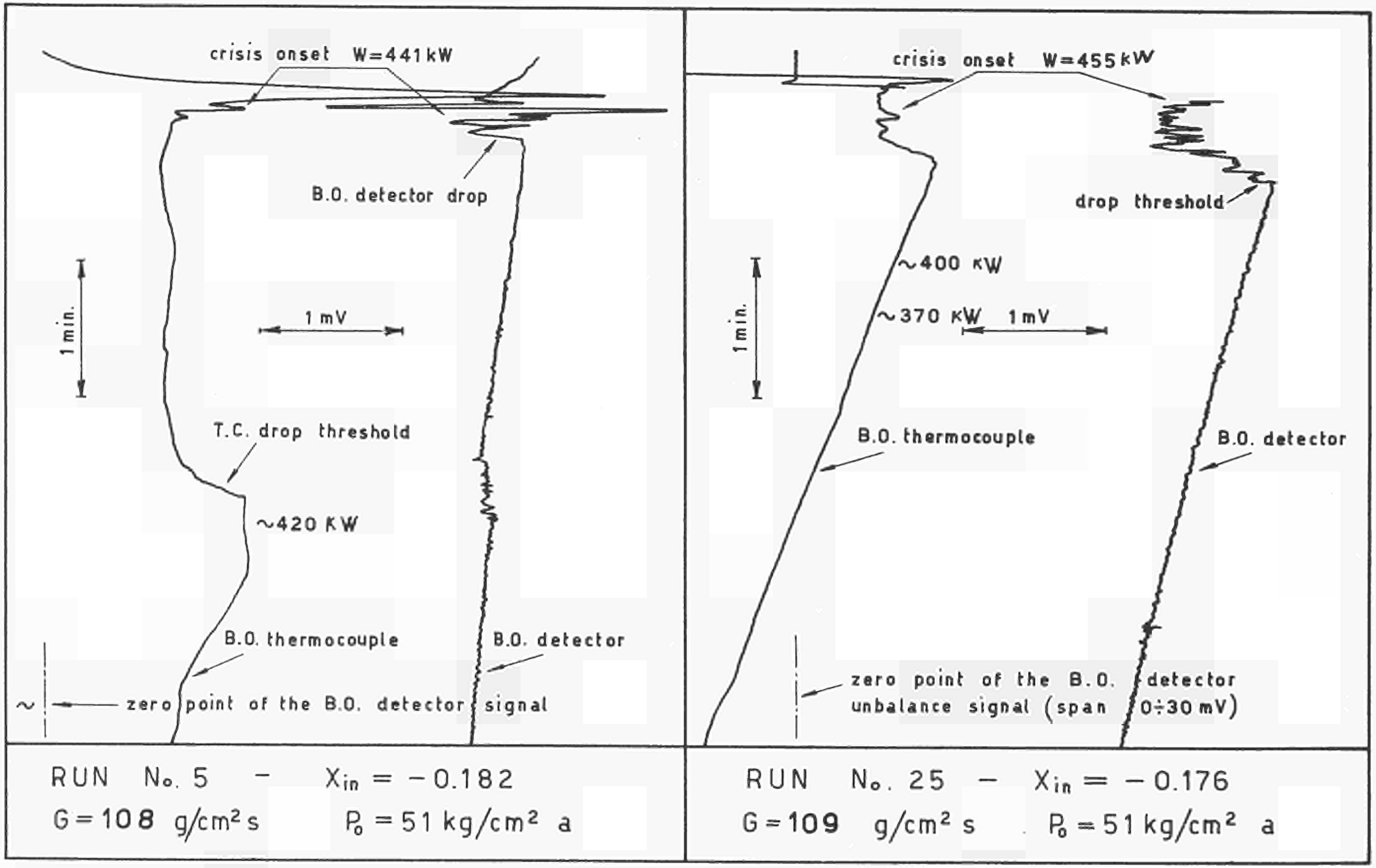

Fig. 20 – Comparison between crisis recordings (EL IT18 – TABLE 3).

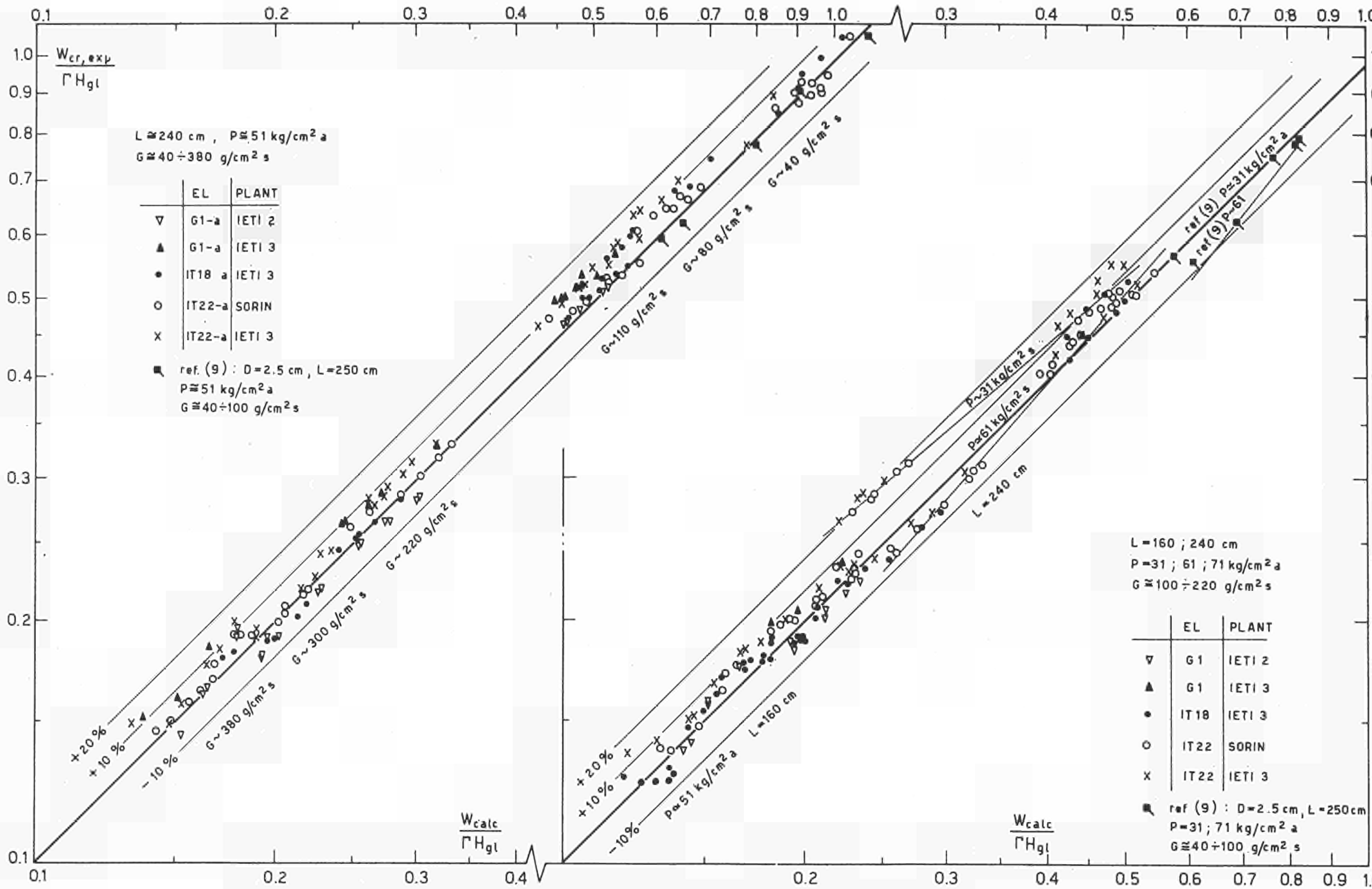

Fig. 21 - Experimental vs predicted critical power data.

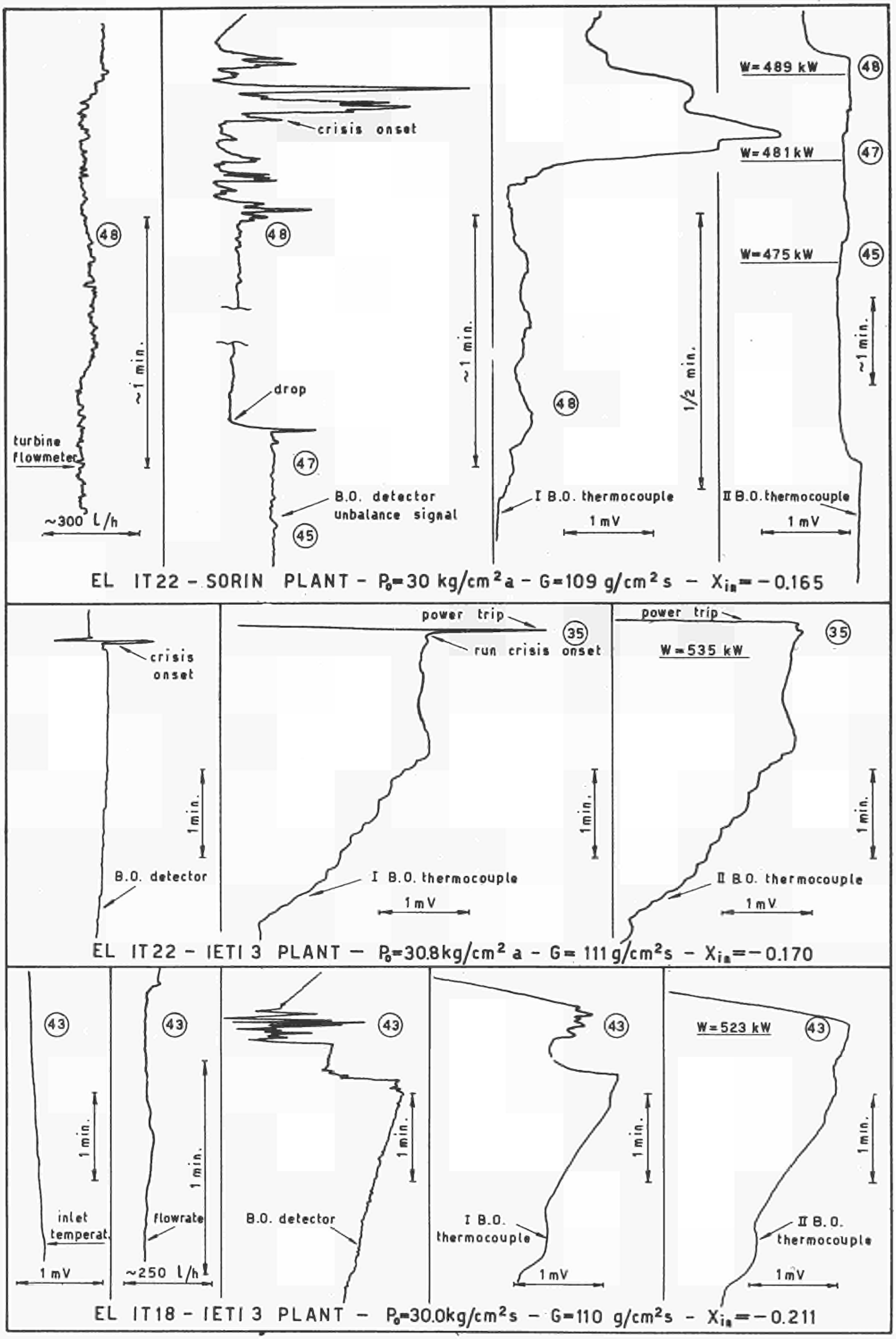

Fig. 22 - Crisis recordings.

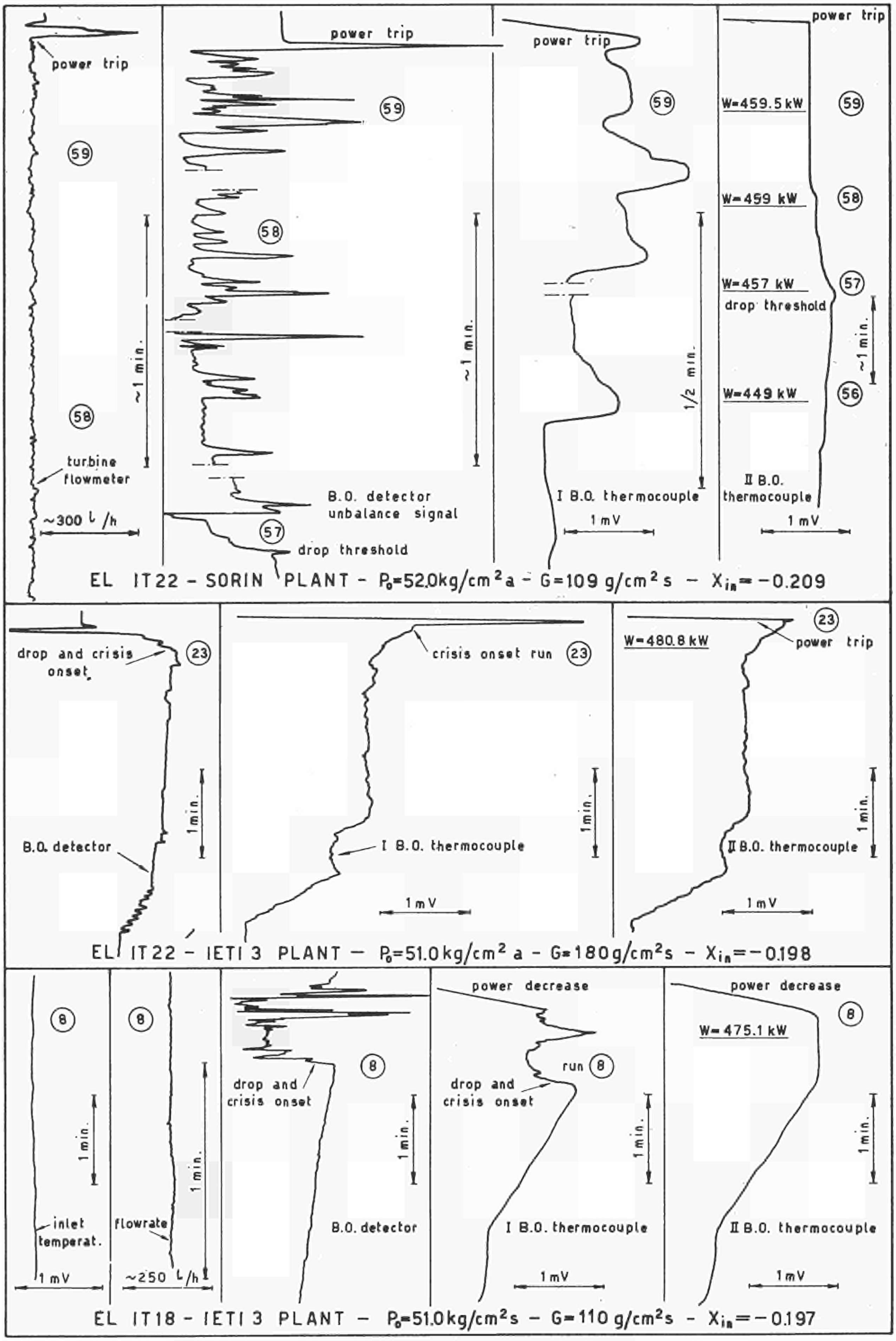

Fig.23 - Crisis recordings.

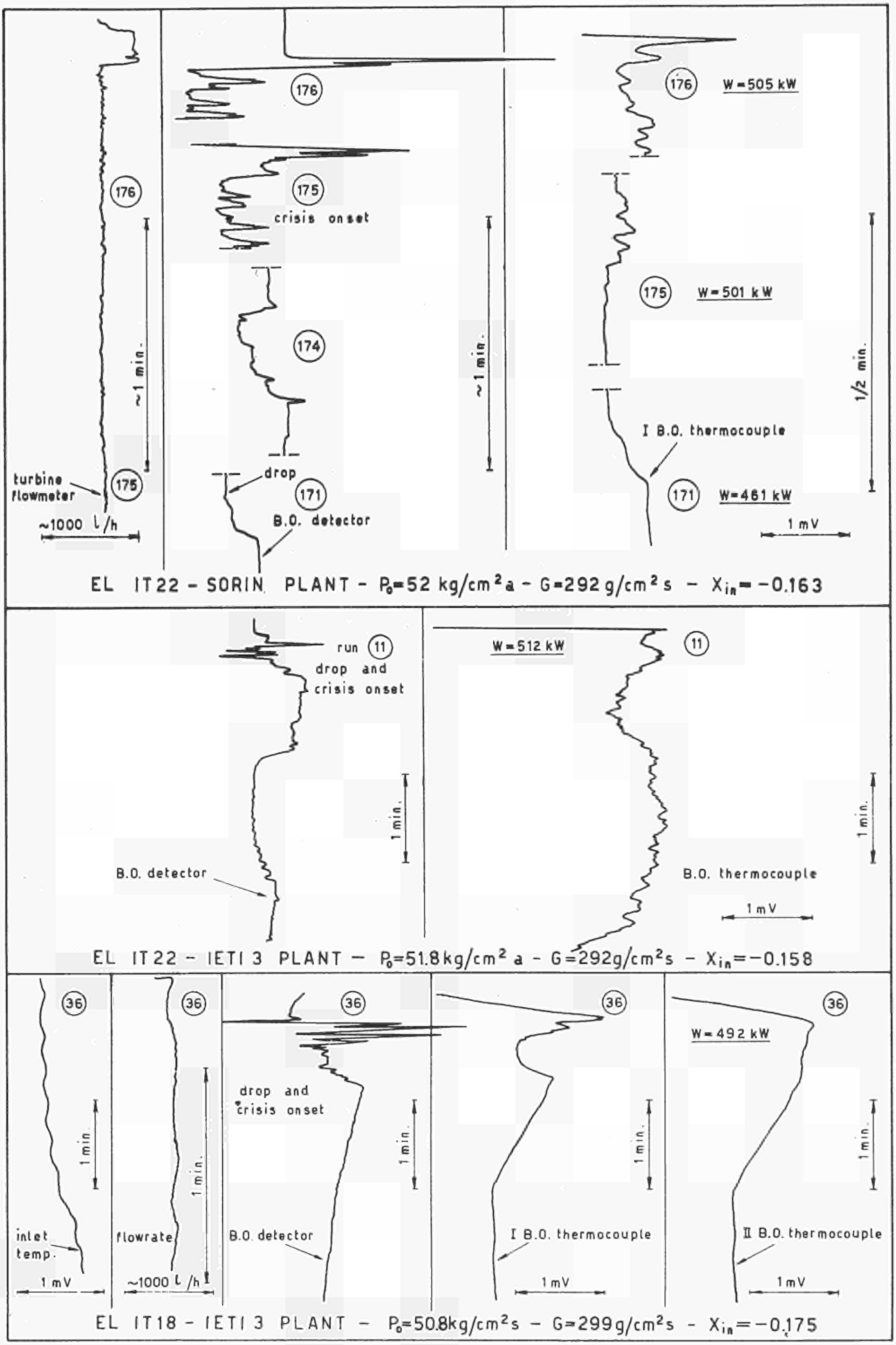

Fig. 24 - Crisis recordings.

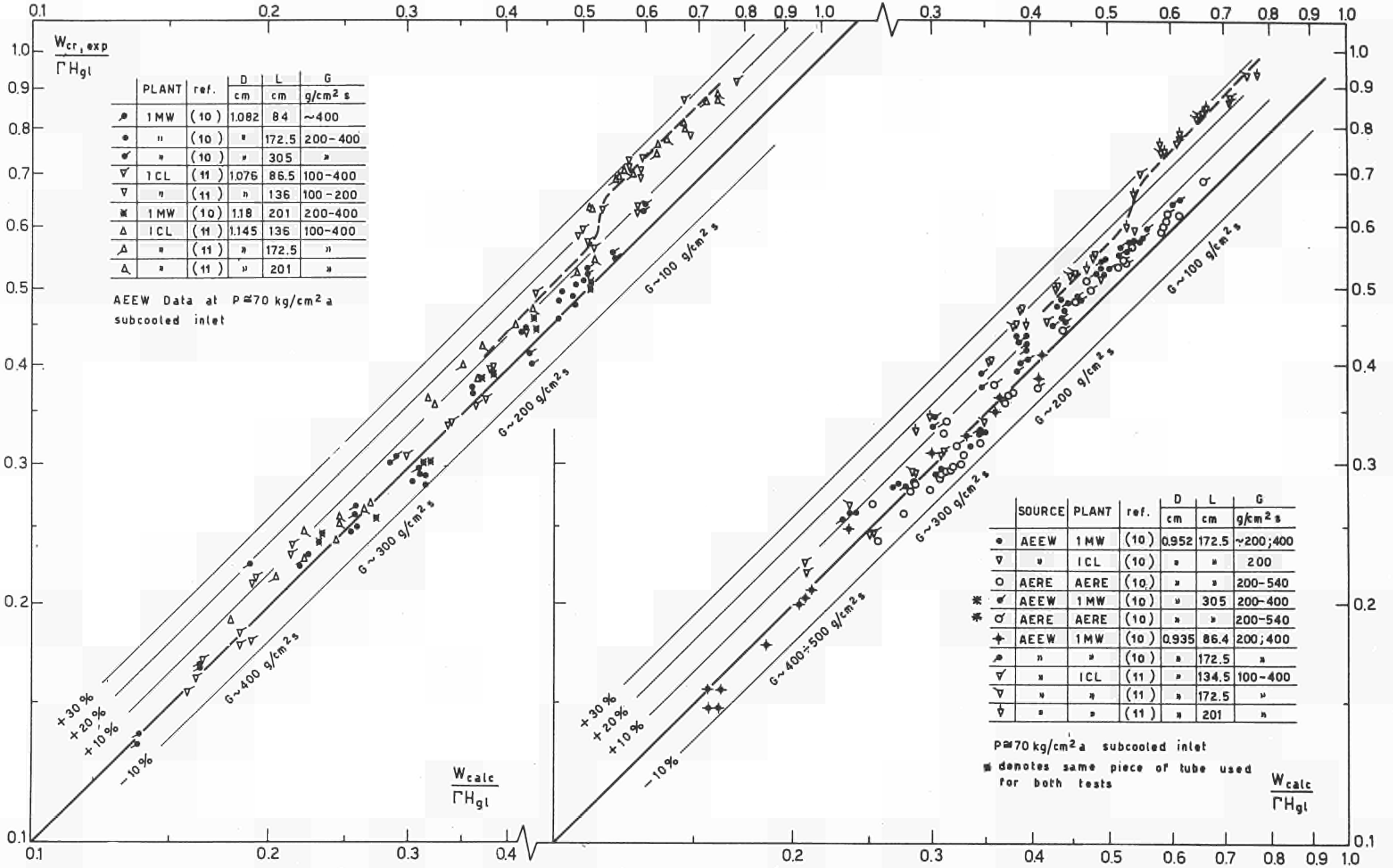

	PLANT	ref.	D cm	L cm	G g/cm² s
●	1 MW	(10)	1.082	84	~400
●	"	(10)	"	172.5	200-400
●	"	(10)	"	305	"
▽	ICL	(11)	1.076	86.5	100-400
▽	"	(11)	"	136	100-200
✱	1 MW	(10)	1.18	201	200-400
△	ICL	(11)	1.145	136	100-400
△	"	(11)	"	172.5	"
△	"	(11)	"	201	"

	SOURCE	PLANT	ref.	D cm	L cm	G g/cm² s
●	AEEW	1 MW	(10)	0.952	172.5	~200;400
▽	"	ICL	(10)	"	"	200
○	AERE	AERE	(10)	"	"	200-540
✱ ●	AEEW	1 MW	(10)	"	305	200-400
✱ ○	AERE	AERE	(10)	"	"	200-540
✦	AEEW	1 MW	(10)	0.935	86.4	200;400
●	"	"	(10)	"	172.5	"
▽	"	ICL	(11)	"	134.5	100-400
▽	"	"	(11)	"	172.5	"
▽	"	"	(11)	"	201	"

Fig. 25 – Experimental vs predicted critical power data.

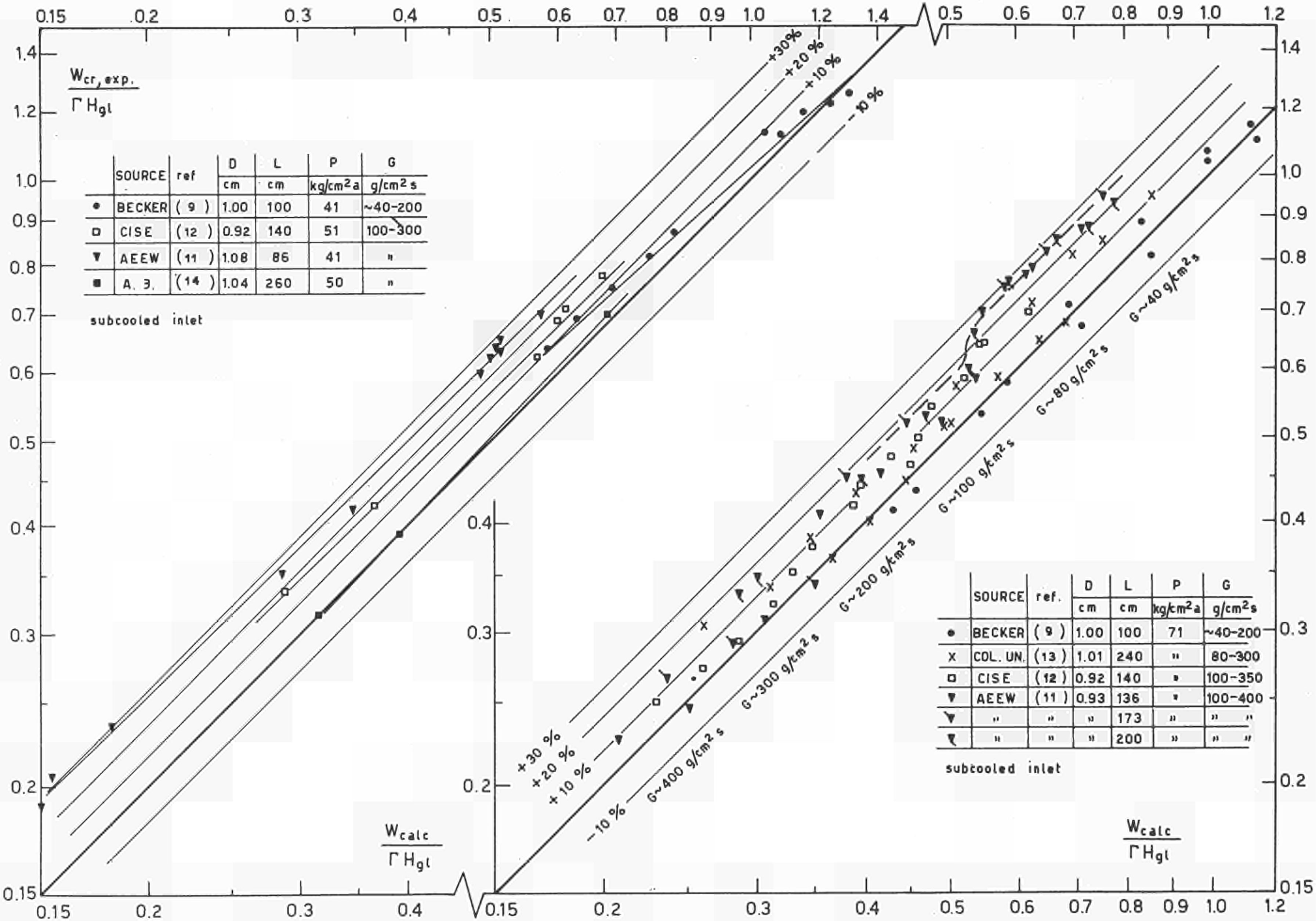

Fig.26 - Experimental vs predicted critical power data.

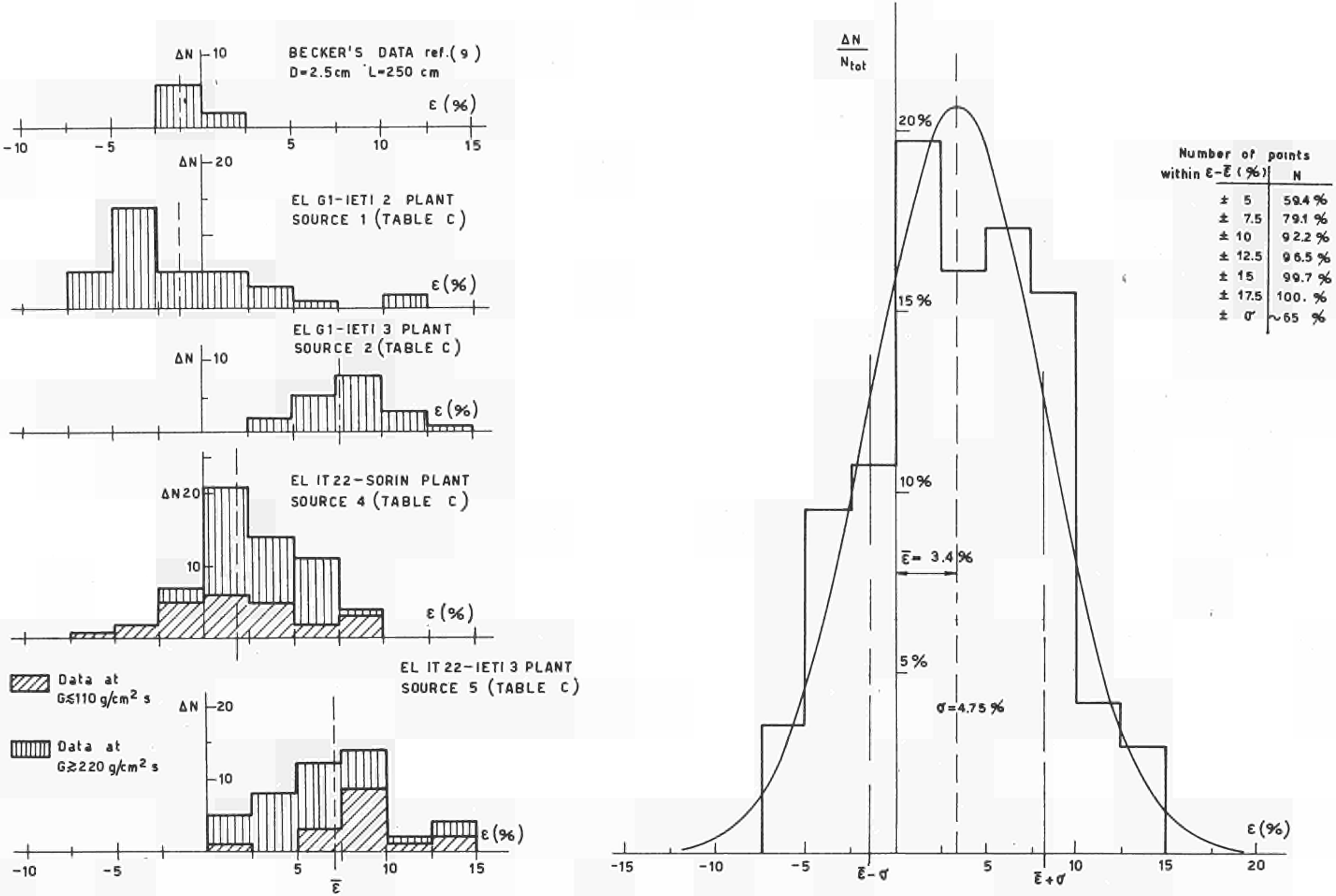

Fig. 27 - Histograms of experimental points vs the deviation from CISE correlation - D=2.5 cm, L=160 and 240 cm, $P \cong 51\ kg/cm^2$, $G \cong 40 \div 380\ g/cm^2 s$; Total number of points: 167 .- Average deviations are derived from table C

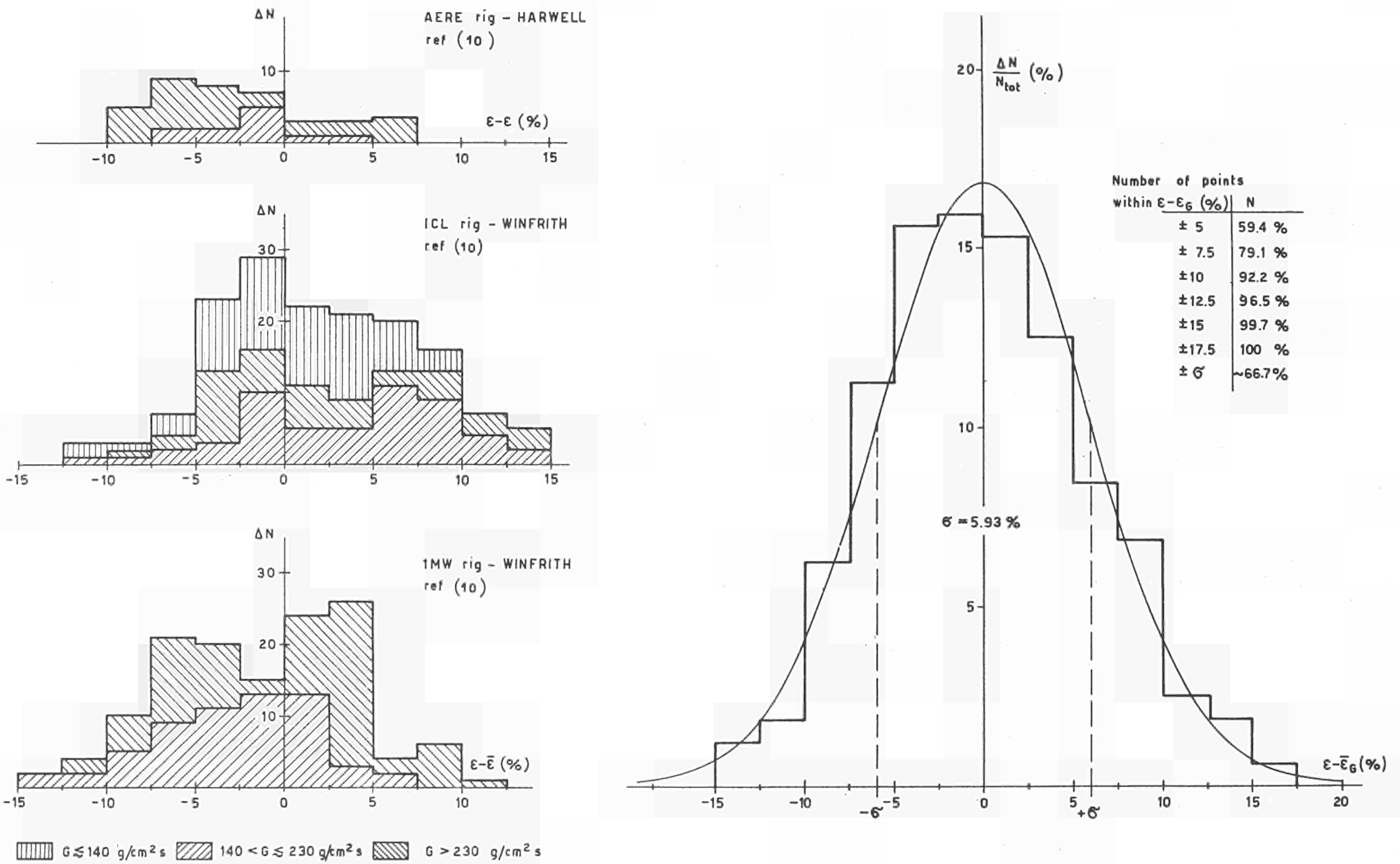

Fig. 2.8 – Histograms of UKAEA experimental points vs the deviation from CISE correlation – $D \cong 0.93-1.2$ cm ; $L \cong 84-305$ cm ; $P \cong 71$ kg/cm² a ; $G \cong 100-500$ g/cm²s – Total number of points : 322.

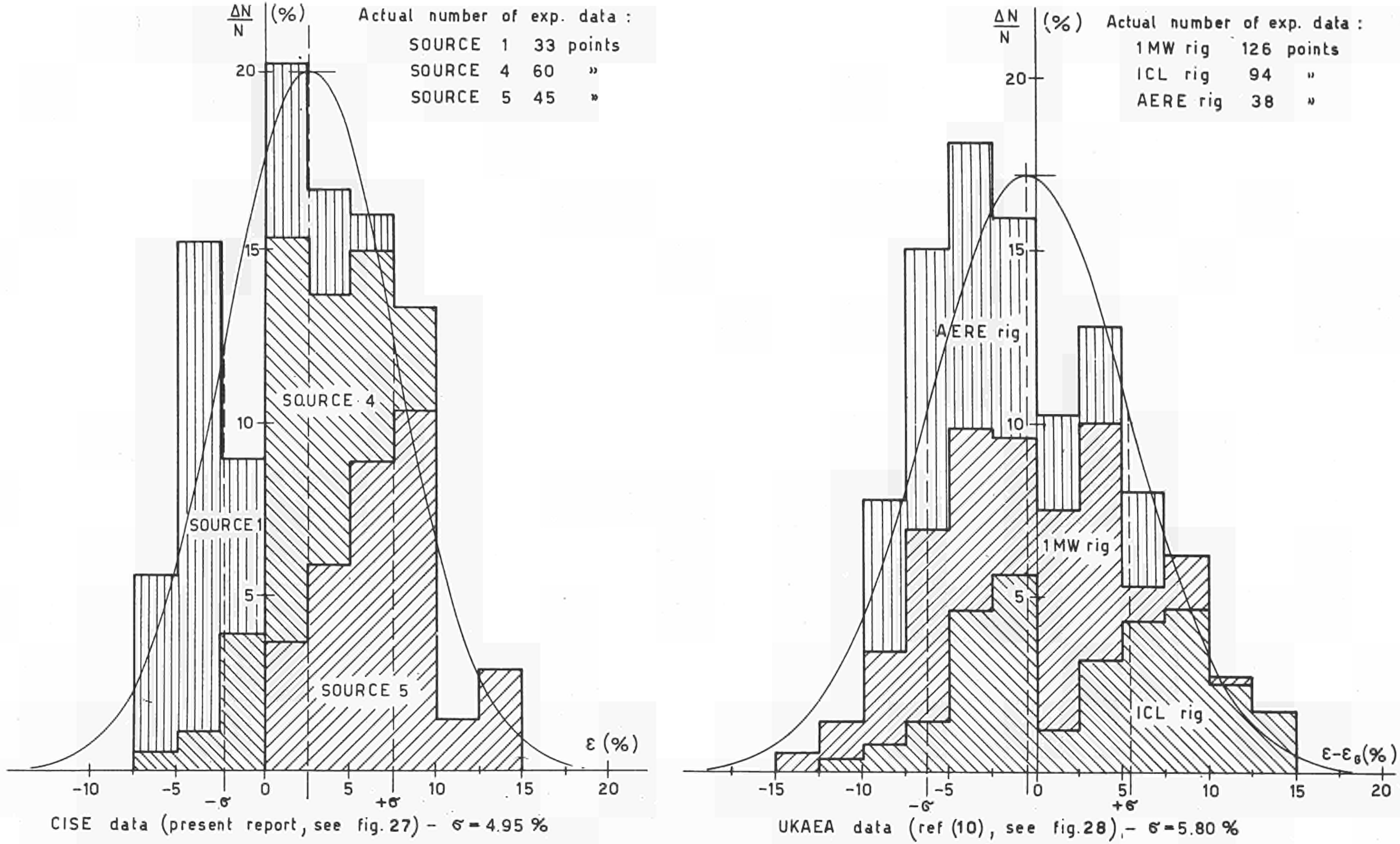

Fig. 29 - Histograms for sources normalized to the same number of points.

NOTICE TO THE READER

All Euratom reports are announced, as and when they are issued, in the monthly periodical **EURATOM INFORMATION**, edited by the Centre for Information and Documentation (CID). For subscription (1 year : US$ 15, £ 6.5) or free specimen copies please write to :

Handelsblatt GmbH
"Euratom Information"
Postfach 1102
D-4 Düsseldorf (Germany)

or

Office central de vente des publications
des Communautés européennes
2, Place de Metz
Luxembourg

To disseminate knowledge is to disseminate prosperity — I mean general prosperity and not individual riches — and with prosperity disappears the greater part of the evil which is our heritage from darker times.

Alfred Nobel

SALES OFFICES

All Euratom reports are on sale at the offices listed below, at the prices given on the back of the front cover (when ordering, specify clearly the EUR number and the title of the report, which are shown on the front cover).

OFFICE CENTRAL DE VENTE DES PUBLICATIONS DES COMMUNAUTES EUROPEENNES
2, place de Metz, Luxembourg (Compte chèque postal Nº 191-90)

BELGIQUE — BELGIË
MONITEUR BELGE
40-42, rue de Louvain - Bruxelles
BELGISCH STAATSBLAD
Leuvenseweg 40-42, - Brussel

DEUTSCHLAND
BUNDESANZEIGER
Postfach - Köln 1

FRANCE
SERVICE DE VENTE EN FRANCE DES PUBLICATIONS DES COMMUNAUTES EUROPEENNES
26, rue Desaix - Paris 15e

ITALIA
LIBRERIA DELLO STATO
Piazza G. Verdi, 10 - Roma

LUXEMBOURG
OFFICE CENTRAL DE VENTE DES PUBLICATIONS DES COMMUNAUTES EUROPEENNES
9, rue Goethe - Luxembourg

NEDERLAND
STAATSDRUKKERIJ
Christoffel Plantijnstraat - Den Haag

UNITED KINGDOM
H. M. STATIONERY OFFICE
P. O. Box 569 - London S.E.1

EURATOM — C.I.D.
51-53, rue Belliard
Bruxelles (Belgique)